# PREDICTIVE LITERATURE ANALYSIS AND IN VITRO EVALUATION OF ADENINE BASE EDITORS TARGETING THE LMNA-Q493X MUTATION IN MURINE FIBROBLASTS

Soumaya Robdon - 7053460
Master Program: Cardiovascular health and disease
August 2024

Daily Supervisor: Elvira den Hertog
Examiner: Prof. Dr. Eva van Rooij
Second Reviewer: Prof. Dr. Catherine Robin
Period: september 2023 – august 2024

Van Rooij Lab

Hubrecht institute

# Abstract

Cardiac laminopathies (LMNA-DCM) are a LMNA-associated subgroup of dilated cardiomyopathy (DCM), and one of the most common types of familiar DCM. LMNA is a gene coding for A-type lamins, which are proteins integral to the structure known as the nuclear lamina. They contribute to nuclear integrity, as well as mechanotransduction and genetic regulation. Currently, there is no cure available for cardiac laminopathies. Gene editing to correct LMNA-DCM causing mutations has provided an approach that could cure laminopathies. However, the heterogenous nature of LMNA mutations and limited data on the safety of targeting them, still poses a challenge. We therefore performed an in-depth literature analysis, collecting potential base editors for the treatment of cardiac laminopathies. We then used available data to predict the compatibility, efficiency, and safety of these editors in targeting the patient-derived LMNA-Q493X mutation. After selecting the editors predicted to be most safe and effective, we constructed them along with their sgRNAs, into lentiviral transfer vectors which we used to produce the lentiviral treatments. We subsequently treated primary murine liver fibroblasts from wildtype ($LMNA^{WT/WT}$), heterozygous- ($LMNA^{WT/Q493X}$) or homozygous mutant ($LMNA^{Q493X/Q493X}$) mice and evaluated the rate of transduction. Following this treatment, levels of *LMNA/C*, *LMNA* and *LMNC* transcripts were quantified. We found that lentiviral particles transduced the cell cultures with varying success, showing lower efficiency of transduction in highly dense cultures. We additionally showed that SpRYCas9-ABE9 with sgRNA3, as predicted by the data analysis, was most consistent in restoring the evaluated transcript levels *in vitro*.

Therefore, this study does not only contribute to the depth and quantity of available data on gene editing in cardiac laminopathies. It additionally sets a precedent for the use of predictive literature analyses in streamlining of the adaptation of gene therapy approaches. This facilitates the realization of gene therapy as a viable treatment option for all individuals suffering from cardiac laminopathies.

# Layman's summary

LMNA is een gen dat codeert voor de eiwitten Lamin A en Lamin C. Deze eiwitten dragen bij aan de vorm en structurele integriteit van alle celkernen in het lichaam. Daarnaast kunnen ze ook een rol spelen in andere cel-processen zoals genetische regulatie en mechanotransductie. Mechanotransductie is het proces waarin een cel fysische krachten die op de cel uitgeoefend worden, om kan zetten in een biologische reactie. Zo kan een cel de stevigheid van zijn kern bijvoorbeeld aanpassen op toenemende krachten. Wanneer LMNA gemuteerd is, leidt het tot een groep aandoeningen, genaamd laminopathieën. Verschillende typen laminopathieën beïnvloeden verschillende organen. Een type laminopathie, namelijk de cardio-laminopathie, beïnvloed de functie van het hart. Dit leidt vaak tot hartfalen, en hartritmestoornissen. Ondanks dat er therapieën beschikbaar zijn die de symptomen kunnen behandelen, is er op dit moment nog geen genezing voor cardio-laminopathieën.

Gentherapie zou een genezende behandeling kunnen vormen voor cardio-laminopathieën. Gentherapie is een verzamelnaam voor therapeutische middelen die een aandoening behandelen door de oorzakelijke mutatie te corrigeren. Een specifieke methode die valt onder 'gentherapie', is een groep enzymen genaamd '*base editors*' (BE). Deze BE's zijn ontworpen om één base aan te passen, en kunnen gebruikt worden wanneer de mutatie maar één nucleotidepaar omvat.

Echter, is het niet mogelijk om deze methoden op dit moment in de kliniek toe te passen. Deze uitdaging wordt veroorzaakt door het feit dat de enzymen die worden gebruikt om de mutatie te corrigeren, verschillend reageren in verschillende regio's van het DNA. De sequentie van het DNA om de mutatie heen, draagt dus bij aan het succes van zo'n BE. En omdat cardio-laminopathieën worden veroorzaakt door vele verschillende mutaties, is er niet genoeg informatie om te weten hoe een BE in al die verschillende regio's zal functioneren. Daarbij is er ook meer informatie nodig over de veiligheid van dit soort enzymen, en de kans dat zij een andere aanpassing aanbrengen dan de bedoelde correctie.

In deze studie, hebben wij een literatuuronderzoek uitgevoerd om te analyseren welke BE's het beste werken in veel genetische regio's. We hebben verschillende eigenschappen van deze BE's genoteerd en daarvan een overzicht gemaakt. Op basis van de eigenschappen die beschikbaar waren, hebben wij vervolgens een voorspelling gemaakt, met betrekking tot de BE's in de selectie die het meest efficiënt en veilig zijn in de regio van de patiënt-specifieke LMNA-Q493X mutatie (Glutamine positie 493 -> stop-codon). Deze mutatie introduceert een stop-codon, zo vroeg in het transcript, dat het mRNA dat hieruit volgt niet kan bijdragen aan een functioneel eiwit. Hierdoor is de concentratie van Lamin A en Lamin C in de cellen die deze mutatie dragen, veel lager dan in gezonde cellen. BE's maken gebruik van zogenaamde '*single-guide-RNAs*' (sgRNA). Dit zijn RNA strengen die complementair zijn aan de regio in het DNA die je wilt modificeren, en helpen met het begeleiden van de enzymen naar de juiste plek. Nadat we de beste sgRNA's hadden geselecteerd voor de genoemde BE's, hebben we ze samen ingepakt in lentivirale deeltjes. Deze virale deeltjes maken je niet ziek, maar kunnen er wel voor zorgen dat de BE's in de cellen terecht komen waar ze nodig zijn. Deze deeltjes hebben wij vervolgens gebruikt om cellen van muizen te behandelen. De cellen hebben we eerder geïsoleerd uit gezonde muizen, muizen die een heterozygote Q493X mutatie hadden, of muizen die een homozygote Q493X mutatie hadden. Om te bevestigen dat de deeltjes met de BE's ook daadwerkelijk in de cellen tot expressie komen, hebben we ook deeltjes gemaakt met de GFP (*green fluoresent protein*). Dit is een eiwit dat groen licht kan uitstralen wanneer het tot expressie komt. Vervolgens hebben we gekeken of de gezonde Lamin A en Lamin C coderende mRNA concentratie weer hersteld was.

We vonden in totaal 32 BE's die positieve kenmerken hadden en dus mogelijk te testen waren. Van die 32 BE's, waren er drie waarvan ook in de specifieke Q493X regio voorspeld werd dat zij het meest efficiënt en veilig waren. Dit bleken de volgende BE's te zijn: SpRYCas9-ABE8e, SpRYCas9-ABE9 en iABE-NGa. Na de behandeling van de geïsoleerde cellen, bleek dat de BE's niet in de cellen van elke muis even goed tot expressie kwamen. Wanneer de dichtheid van de cellen in het schaaltje waarin ze groeien te hoog was op de dag van de behandeling, kwamen de GFP-deeltjes

minder goed tot expressie. Verder blijkt uit ons onderzoek dat van de BE-sgRNA combinaties, de combinatie SpRYCas9-ABE9 met sgRNA 3 het meest consistent is in het herstellen van de mRNA concentratie. Dit is ook wat wij voorspelden op basis van de informatie die beschikbaar was uit andere studies.

Deze studie draagt dus bij aan de toename van informatie over BE's, met betrekking tot hun effectiviteit in het behandelen van cardio-laminopathie-gerelateerde mutaties. Bovendien laat het zien dat het meenemen van een voorspelling betreffende de efficiëntie en veiligheid van de BE's in de regio in het DNA die je wilt corrigeren, het makkelijker kan maken om deze methode aan te passen op de vele verschillende mutaties. Dit kan tijd en middelen besparen in het ontwikkelen van nieuwe gentherapieën voor cardio-laminopathieën. Kortom, door deze studie, zijn we een stap dichter bij het gebruik van genezende behandelingen voor cardio-laminopathieën.

# Abbreviation list

| | | |
|---|---|---|
| 8e.1 | - | SpRY-ABE8e+sgRNA1 |
| 8e.2 | - | SpRY-ABE8e+sgRNA2 |
| 8e.3 | - | SpRY-ABE8e+sgRNA3 |
| 8e.4 | - | SpRY-ABE8e+sgRNA4 |
| 9.3 | - | SpRY-ABE9+sgRNA3 |
| 9.4 | - | SpRY-ABE9+sgRNA4 |
| A | - | Adenine |
| AAV | - | Adenovirus-associated virus |
| ABE | - | Adenine base editor |
| ACE | - | Angiotensin-converting enzyme |
| ANOVA | - | Analysis of variance |
| BE | - | Base editor |
| C | - | Cytosine |
| Cas | - | CRISPR-associated |
| CBE | - | Cytosine base editor |
| cDNA | - | Complementary DNA |
| CM | - | Cardiomyocyte |
| $CO_2$ | - | Carbon dioxide |
| CRISPR | - | Clustered regularly interspaced short palindromic repeats |
| D12f | - | nuclease deactivated Un1Cas12f1 |
| DCM | - | Dilated cardiomyopathy |
| DMEM | - | Dulbecco's modified eagle medium |
| DNA | - | Deoxyribonucleic acid |
| EDMD | - | Emery-Dreifuss muscular dystrophy |
| FBS | - | Foetal bovine serum |
| G | - | Guanine |
| GFP | - | Green fluorescent protein |
| $H_2O$ | - | Hydrogen dioxide |
| HEK | - | Human embryonic kidney |
| HEPES | - | 2-(4-(2-hydroxyethyl)-1-piperazinyl)-ethane sulfonic acid |
| HET | - | Heterozygous mutant |
| HGPS | - | Hutchinson-Gilford progeria syndrome |
| hiPSC | - | Human induced pleuripotent stem cells |
| hiPSC-CM | - | hiPSC derived cardiomyocytes |
| HOM | - | Homozygous mutant |
| iABE-NGa | - | miniABE-SpCas9-NGa |
| ICD | - | Implantable cardioverter-defibrillator |
| iNGa.4 | - | iABE-NGa+sgRNA4 |
| LAD | - | Lamina-associated domain |
| LINC | - | Linker of nucleoskeleton and cytoskeleton |
| LMNA | - | Lamin A/C (gene) |
| *LMNA* | - | Lamin A transcript |
| LMNA-DCM | - | Cardio-laminopathy |
| *LMNA/C* | - | Lamin A/C transcripts |
| *LMNC* | - | Lamin C transcript |
| LV | - | Lentivirus |

| | | |
|---|---|---|
| MAPK | - | Mitogen-activated protein kinase |
| mRNA | - | Messenger RNA |
| mTOR | - | Mammalian target of rapamycin |
| nTPM | - | Normalized transcripts per million |
| PAM | - | Protospacer adjacent motif |
| PCR | - | Polymerase chain reaction |
| POLR2A | - | RNA polymerase II subunit A |
| qPCR | - | Quantitative PCR |
| RNA | - | Ribonucleic acid |
| s.e.m. | - | Standard error of mean |
| sgRNA | - | single guide RNA |
| ssDNA | - | Single strand DNA |
| SUN1 | - | SUN domain-containing protein 1 |
| T | - | Tyrosine |
| TadA | - | Transfer RNA deaminase |
| WT | - | Wildtype |

## Introduction

Cardiac laminopathies (LMNA-DCM) are a subgroup of dilated cardiomyopathies (DCM) that are caused by a pathological mutation in the LMNA gene (1). Of the estimated 1 in every 250 individuals that experience DCM, up to 50% has a genetic cause. Of the number of patients with familial DCM, up to 8% is a result of a LMNA mutation, making it one of the most common genetic DCM causes (2,3). All individuals carrying such a mutation, experience symptoms by the age of 60 indicating an age-related full penetrance (1). DCM characteristically portrays left ventricular dilation and dysfunction in the heart. With cardiac laminopathies in particular, these signs are accompanied by cardiac conduction defects, and skeletal muscle deficits(1). Interestingly, the heterogeneity seen in the clinical presentation of this disease, both in age of onset and symptoms, is vast (4). Upon onset, the prognosis is poor in comparison to other types of familiar DCM, with LMNA mutation carrying DCM patients having an increased rate of mortality, transplantation, and occurrence of major cardiac events compared to non-LMNA mutation carrying DCM patients (5). Apart from that, the mortality rate of cardiac laminopathy patients is up to 4 times as high as the standard population (6).

The LMNA gene codes for A-type lamins. A-type lamins are filamentous proteins that contribute to, and reinforce, the structural integrity of the nuclear lamina. The nuclear lamina is part of the nuclear envelope, a structure that encompasses the nuclear contents (7). A-type lamins typically have a genetic structure that can be divided into a head-, coil-, and tail domain.
Lamin A and Lamin C are the two isoforms that can be produced from transcripts of the LMNA gene(8). The distinction between these isoforms can be made based on their tail domain. Lamin A, through alternative splicing, includes exons 11 and 12, which are absent in Lamin C. This leads to Lamin A containing a longer tail domain that includes a C-terminal CaaX motif. This motif enables the post-translational processing of Lamin A (9). Lamins A and C self-assemble to form the nuclear lamina (10,11).
In addition to the reinforcement of the nuclear envelope, Lamins A and C impact both mechanotransduction- and genetic regulatory pathways. Mechanotransduction entails the adaptation of cellular processes in response to mechanical stresses that act on the cell (12). The nuclear lamina can relay signals from outside the cell through the linker of nucleoskeleton and cytoskeleton (LINC) complex (13), and use them to regulate durability (14), cellular identity (15), and other features of cellular function. This process can be facilitated by the regulation of gene expression (12). A-type lamins can for example bind to lamina associated domains (LADs) in the chromatin to rearrange it or restrict its movement (16,17). Additionally, they can bind proteins to enact DNA-protective and DNA-regulatory features (18,19). In summary, A-type lamins are a group of proteins essential for cellular durability and adaptability to mechanical stresses.
Mutations in this gene therefore affect many different cellular processes, primary related to structural integrity, mechanotransduction, and gene regulation. Mutations in LMNA can for instance result in nuclear deformity and disruption leading to an increase in apoptosis and desmin mislocalization, as described by Nikolova et al. (20). Additionally, LMNA mutation leads to altered mechanotransduction. Chen et al. reported that LMNA mutations can impact levels of the LINC complex protein SUN1 leading to its accumulation and disruption of nuclear functions (21). Furthermore, as described by Mounkes et al., mutations in the LMNA gene can cause mislocalization of connexins, which normally assemble to form gap junctions essential for electrical signal conduction in the heart (22). This is potentially a consequence of disturbed cytoskeletal dynamics, as shown in a study conducted by Macquart et al (23). Moreover, as described by multiple studies, LMNA mutations influence the localization of the earlier mentioned LADs in a mutation-specific manner. This feature not only influences genetic expression directly, but also rewrites the epigenetic profile of certain regions of the genome (24–26). Other ways in which LMNA mutation influences genetic expression, are through the

interactions with gene regulatory proteins, and proteins from numerous signaling cascades, including the MAPK and mTOR signaling pathways (27–30).

Currently, standard practice in the treatment of cardiac laminopathies focuses on managing symptoms. In addition to drugs like ACE inhibitors and beta blockers, the implantation of an implantable cardioverter defibrillator (ICD) can be considered. However, while heart transplantation is the only resolving treatment type, it is not curative (4). All of these treatment options carry considerable risks ranging from bradycardia, to graft failure and mortality (4,31,32). Novel treatment options target signaling pathways affected by LMNA mutations, such as mTOR and MAPK signaling cascades, which are hyperactivated upon LMNA mutation (28,33,34). The aim of these therapies is to reverse the hyperactivation and alleviate or manage symptoms (34,35). Recently, a promising variant of this type of pharmacological therapy, had been ARRY-371797 (a selective p38alfa MAPK inhibitor), as it showed improvements of functional capacity in phase 2 trials (36). However, the phase 3 REALM-DCM trial was terminated early after failure to produce a significant effect (37). A potential reason for the lack of clinical success for this type of treatment, could be the fact that a singular process is being targeted, while LMNA mutation alters a significant range of processes. To combat the many facets of LMNA-DCM, there is therefore a dire need for a curative approach to cardiac laminopathies, that targets the issue at the source.

A potential approach that accomplishes this, is the application of gene editing. There is, however, limited data concerning gene editing therapies in cardiac laminopathies. The types of mutations found in LMNA-DCM can be very heterogenous leading to a vast diversity of potential gene therapy approaches. A few examples that have been studied, are the direct classical CRISPR-Cas approach to mutation as shown in the study conducted by Salvarani et al (38). Additionally, the replenishing of Lamin A/C levels through transgenic expression in a knockout model of LMNA has been studied(39). Furthermore, exon skipping is an approach with considerable potential in combatting missense mutations, by skipping the exon with the pathological mutation (40). Most of these attempts have had a set-up in which a proof-of-concept had been achieved, but few formed a solid basis to develop treatments. For this to be feasible, there needs to be more data on the safety profile of genetic editing approaches in the LMNA context, when trying to edit LMNA-DCM specific mutations *in vivo*. This is essential to prevent the unintended introduction of a potentially pathological mutation. The limited data currently available predominantly focuses on the efficiency of editing and to a smaller degree on the restoration of cellular- and cardiac function, though data on these topics is scarce as well.
There have however been numerous reports of gene editing, specifically base editing, of other inherited cardiomyopathies, including other DCM mutations. These reports do include an analysis into off-target effects and delivery (41–45). Adenine base editing (ABE) is a type of gene editing that modifies a single nucleotide from an adenine (A) to a guanine (G), changing the base pair from an A-T to a G-C basepair (46). The group of ABEs were developed, inspired by the mechanism of the already existing cytosine base editors (CBEs). As a single stranded DNA (ssDNA) adenine deaminase does not naturally occur, directed evolution of a transfer RNA deaminase (TadA) was used to develop ABE 7.10 as reported by Gaudelli et al. in 2017 (47).
Since 2017, ABE7.10 has been improved upon several times. Different Cas9 and deaminase variants have been combined and modified over the past 6-7 years to develop base editors with more favorable properties. On top of that, deep learning based computational tools have been developed, that can predict the suitability of different base editors and guide RNAs for a specific locus. These tools, such as DeepABE, facilitate the characterization of the adenine base editing landscape around a target locus, using fewer experiments (48). Recently a study reported by Yang et al. described a murine model in which they used DeepABE to predict the efficiency of multiple single guide RNAs in restoring a point mutation through adenine base editing in LMNA, with low rates of bystander editing. Then, they compared a small selection of different deaminases, Cas9 variants and delivery systems, in their impact on *in vivo* editing efficiencies. The predicted degree

of editing in the target adenine compared to the bystander adenines, correlated considerably with the *in vivo* measured pattern of efficiencies. With this, they underlined the potential within the LMNA locus, of predictive analytics and their use in the development of a base editing approach (49).

Experiments performed in the lab prior to this study, showed a haploinsufficiency of both *LMNA* and *LMNC* transcripts in Q493X heterozygous mutant (LMNA$^{WT/Q493X}$) human induced pluripotent stem cell derived cardiomyocytes (hiPSC-CMs) (Fig. 1a, b). Additionally, reduced Lamin A and Lamin C protein levels were shown (Fig. 1c) and nuclear roundness, a measure for normal nuclear morphology, was reduced in these mutant hiPSC-CMs (Fig. 1d). Upon treatment with an adenine base editor (iABE-NGa), evidence of a degree of editing was found (Fig. 1e), and the samples portrayed a recovery in *LMNA* and *LMNC* transcript levels (Fig. 1e).
In this study, we aim to analyze, select, and predict the most suitable and safe combinations of adenine base editors and their associated guides. We selected base editors and guides that are effective, with a low chance of bystander editing. We then aimed to determine which of the selected combinations is most effective in restoring baseline *LMNA/C* transcription levels in primary murine fibroblasts. We hypothesize that at least one of the selected combinations will restore this feature significantly more effectively than the other combinations. To this end, we treat cultured murine liver fibroblasts from wildtype (LMNA$^{WT/WT}$), heterozygous mutant (LMNA$^{WT/Q493X}$), and homozygous mutant (LMNA$^{Q493X/Q493X}$) mice with all the selected base editor constructs, and we analyze *LMNA/C*, *LMNA* and *LMNC* mRNA levels in the isolated RNA using quantitative polymerase chain reaction (qPCR) analysis. In this study, the restoration of the level of these transcripts is taken as a readout measure for editing efficiency. We found that base editors SpRYCas9-ABE8e, SpRYCas9-ABE9 and iABE-NGa were predicted to be most efficient in editing the mutation while minimizing bystander editing based on previous data. We were able to design respectively four, two and one sgRNAs that fulfilled those requirements. Finally, we found that of the combinations of base editors with guides, SpRYCas9-ABE9 with sgRNA 3 was most effective in consistently restoring *LMNA/C*, *LMNA* and *LMNC* expression levels.

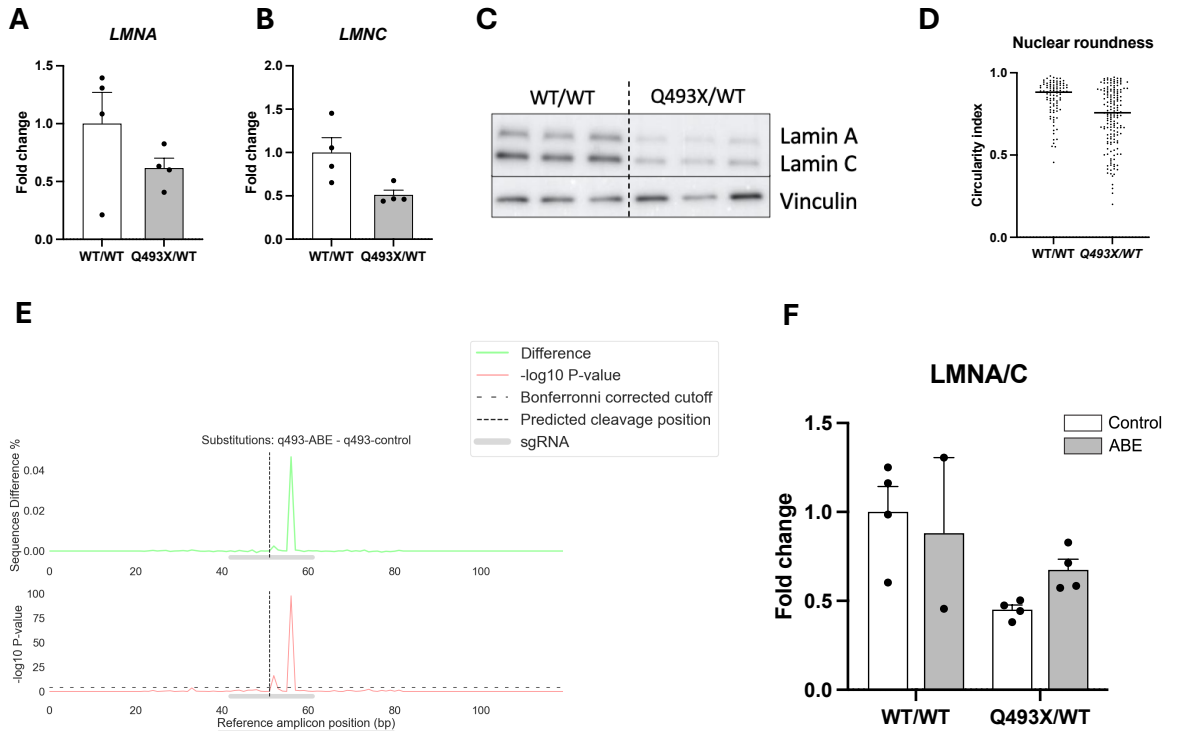

***Figure 1 iABE-NGa base editing of LMNA to restore the LMNA/C mRNA levels in Q493X mutant hiPSC-CMs.* A)** *LMNA* mRNA transcript levels in wildtype (WT/WT) and heterozygous mutant (Q493X/WT) hiPSC-CMs. B) *LMNC* mRNA transcript levels in WT/WT and Q493X/WT hiPSC-CMs. C) Lamin A and C protein levels in WT/WT and Q493X/WT hiPSC-CMs. D) Nuclear circularity in WT/WT and Q493X/WT hiPSC-CMs. E) Graph illustrating the percentage in sequence difference between an untreated and iABE-NGa treated sample of mutant (Q493X/WT) hiPSC-CMs, at different positions in a selected amplicon. This difference indicates the degree of modification of the target base. F) *LMNA/C* total mRNA transcript levels WT/WT and Q493X/WT hiPSC-CMs, treated with either a control, or with iABE-NGa.

# Materials and methods

## Restriction enzyme cloning

To produce iABE-NGa c-terminal and n-terminal intein lentiviral transfer plasmids, the base editor constructs were PCR amplified from their original plasmids (appendix 1 and 2; as present in the lab) using primers that contained overhangs compatible with AgeI and XhoI restriction enzymes (Supp. Table 1). These PCR amplicons were subsequently restricted using AgeI (NEB R3552) and XhoI (NEB R0146) restriction enzymes and ligated into (AgeI and XhoI) restricted lentiviral transfer vector backbones (pLVX-) using T4 DNA ligase (NEB M0202). This resulted in the lentiviral transfer vectors pLVX-iABE-NGa-C-term and pLVX-iABE-NGa-N-term.
pLVX-SpRY-Cas9- C-term, pLVX-SpRY-Cas9-ABE8e- N-term and pLVX-SpRY-Cas9-ABE9-N-term inteins were available from our inventory and produced in previous experiments.
Subsequently, sgRNAs were cloned into all lentiviral transfer plasmids through T4 DNA ligation between BsmBI-v2 (NEB R0739) restricted transfer plasmid backbones and sgRNA-oligo's containing compatible overhangs. The plasmid maps can be found in appendix 3 to 7.
All ligations were transformed into DH5$\alpha$ competent cells, and DNA was extracted and purified using a Purelink Quick Plasmid Miniprep Kit (Invitrogen: K210011). Samples were sent for Sanger sequencing to confirm successful cloning of sgRNA's (Supp. Fig.2), and to confirm sequence alignment to desired constructs (sequencing primers: Supp. Table 3).

## Lentiviral production and titer determination

Human embryonic kidney (HEK)293T cells were seeded in 100mm dishes and passaged 24hrs before lipofectamine 3000 (CAT: L3000015) transfection. Six hours after transfection, the medium was refreshed. 48 hours after transfection, the virus containing medium was collected and filtered (Carl Roth, 0.45um (KH55.1)) and subsequently stored at -80°C. To produce the different lentiviral particles, 7ug of the transfer plasmid (appendix 3-7) was combined with 3ug of a lentiviral envelope plasmid (pMD2G: appendix 8) and 8ug of a lentiviral packaging plasmid (psPAX2: appendix 9). This resulted in experimental lentiviral particles (LV) containing pLVX-SpRY-Cas9-C-term intein with sgRNA 1, 2, 3 or 4, pLVX-SpRY-Cas9-ABE8e-N-term intein with sgRNA 1, 2, 3 or 4, pLVX-SpRY-Cas9-ABE9-N-term intein with sgRNA 3 or 4, pLVX-iABE-NGa-C-term intein with sgRNA 4 and pLVX-iABE-NGa-N-term intein with sgRNA4. Additionally, a reporter lentivirus (LV-GFP) was produced.
Lentiviral titer was determined using Lenti-X qRT-PCR titration kit (TAKARA Bio: 631235) after isolation using Nucleospin Viral RNA isolation (Macherey-Nagel: 740956.50) (supp. Table 4).

## Fibroblast isolation

Murine liver tissue was dissected from wildtype ($LMNA^{WT/WT}$), heterozygous mutant ($LMNA^{WT/Q493X}$) and homozygous mutant ($LMNA^{Q493X/Q493X}$) BI6N mice and homogenized. Samples were digested in DMEM (Gibco:11965092) supplemented with 1% HEPES (Sigma:12103C), 10% Liberase TL (Roche: 54401020001) and 2% DNAse (Worthington: LK003172) using a dissociator (gentleMACS). The cells are subsequently strained (GBO, 70 um (542070). Cells were then neutralized, washed and resuspended with DMEM supplemented with 10% FBS.

## Cell culture

HEK293T cells were cultured in DMEM and transferred to Opti-MEM (Gibco: 11058021) for lipofectamine 3000 transfection.
Primary murine fibroblasts were cultured in DMEM supplemented with 5% FBS and 0,2% primocin (invivogen: ant-pm-1). All cells were cultured at 37°C in a humidified environment with 5% $CO_2$.

## Lentiviral transduction and reporting

Primary murine liver fibroblasts were counted using a cell counter and 40,000 cells were seeded per well on 12-well plates. Samples from every individual mouse were seeded on a separate plate. One well per plate was subjected to LV-GFP reporter lentivirus for further transduction analysis. The remaining wells were subjected to one of the treatment options at a dose of 1000 viral genomes per cell. This includes the combination LV-SpRY-Cas9-Cterm+LV-SpRY-Cas9-ABE8e-Nterm (1000 viral genomes per intein per cell) with sgRNAs 1, 2, 3, or 4, as well as the combination LV-SpRY-Cas9-Cterm+LV-SpRY-Cas9-ABE9-Nterm (1000 viral genomes per intein per cell) with sgRNAs 3 or 4, and the combination LV-iABE-NGa-Cterm+ LV-iABE-NGa-Nterm (1000 viral genomes per intein per cell) with sgRNA 4. The remaining 4 wells were used as untreated control samples. Virus particles were suspended in DMEM supplemented with 5% FBS and 0,2% primocin. Cells were refreshed every 48 hours with DMEM supplemented with 5% FBS and 0,2% primocin. Cells were incubated at 37°C in a humidified environment with 5% $CO_2$. On days 0, 3 and 7 images were taken to indicate cell density prior to treatment using the brightfield channel and rate of transduction using the GFP channel (life technologies EVOS-FL: 12-563-460).

## RNA isolation and quantitative polymerase chain reaction analysis

On day 7 of treatment, total RNA was extracted from samples using TRIzol reagent (Invitrogen: 15569-026/018). Chloroform (BOOM: 76025322.2500) was used to separate RNA containing aqueous phase from DNA and organic material. Isopropyl alcohol (Macron fine chemicals: 15518744) was used to precipitate RNA, which was subsequently washed with 70% ethanol (BOOM: 84010059.500). RNA samples were then resuspended in RNAse free $H_2O$ (Macherey-Nagel: 740378.1000) and concentration was measured using a microvolume spectrophotometer (NanoDrop-2000). Following this the single stranded RNA samples are used to synthesize cDNA using an iscript cDNA synthesis kit (Bio-Rad: 1708891).
Quantitative polymerase chain reaction (qPCR) analysis was performed using iQ SYBR Green supermix (Bio-Rad:1708885), and analyzed using a CFX384 Touch Real-Time PCR System (Bio-Rad:1855484). LMNA/C total, LMNA and LMNC specific primers were used to target these transcripts (supp.Table.2). RNA Polymerase II subunit A (*POLR2A*) was used as a housekeeping gene to normalize cDNA content between samples. *LMNA/C* total, *LMNA* and *LMNC* relative expression for each condition was normalized to the relative expression shown in the wildtype samples subjected to the same experimental condition.

## Statistical analysis

Statistical analysis was performed using PRISM (GraphPad Version 10.2.3). Data is presented as mean +/- s.e.m. ($n \leq 3$). Data was transformed using sin(Y) (*LMNA/C* tot relative expression), $\sqrt{Y}$ (*LMNA* relative expression) and log(Y) (*LMNC* relative expression) transformations, to improve normality and homoscedasticity of residuals and allow appropriate statistical tests (Supp. Fig. 1). An analysis of variance (ANOVA) was performed to test statistical significance. The threshold for statistical significance was $\alpha$=0,05.

| Deaminase | Cas-enzyme | PAM sequence | Editing window | Optimal protospacer length | Optimalisation (in comparison to SpCas9-ABE7.10) | Delivery method *in vivo* | Model in original article | | Source |
|---|---|---|---|---|---|---|---|---|---|
| | | | | | | | *In vitro*: | *in vivo*: | |
| **ABE7.10** | SpCas9 | NGG | 4-7 | 20 | - | - | HEK293T cells | | (47) |
| **ABE7.10** | xCas9 | NG, GAA, GAT | 4-8 | 20 | Improved PAM applicability | - | HEK293T cells | | (50) |
| **ABE7.10** | KKH-SaCas9 | NNNRRT R= purines | 3-14 (highly active 8-13) | 20 | Improved PAM applicability, reduced size | RNA mixture injected into zygote | HEK293T cells | Mouse /Rat embryos | (51,52) |
| **ABE7.10** | VQR-Cas9 | NGA | ~3-8* | 20 | Improved PAM applicability | RNA mixture injected into zygote | HEK293T cells | Mouse/ Rat embryos, Zebrafish | (51,53) |
| **ABEmax** | SpCas9 | NGG | 4-7 | 20 | Improved efficiency | - | HEK293T cells, patient derived fibroblasts, N2A cells | | (54) |
| **ABEmax** | exCas9 | NGG, NGA, NGT | | 20 | Improved efficiency regardless of genomic site | RNA mixture injected into zygote | | Rabbit embryos | (55) |
| **ABEmax-AW** | SpCas9 | NGG | 4-8 | 20 | Reduced off target editing | - | HEK293T cells/ HeLa cells | | (56) |
| **ABE7.10-F148A** | SpCas9 | NGG | ~4-6* | 20 | Reduced off target editing | - | HEK293T cells | | (57) |
| **SECURE-ABE's** | SpCas9 | NGG | 4-7 | 20 | Reduced RNA off target editing, reduced size | - | HEK293T cells/ HepG2 cells | | (58) |
| **ABE8e** | SpCas9 | NGG | 4-8 | 20 | Reduced size, Improved Cas enzyme applicability, Improved efficiency | - | HEK293T cells | | (59) |
| **ABE8e** | SaCas9 | NNGRRT | 3-14 | 22 | Reduced size, Improved PAM applicability | - | HEK293T cells | | (59) |
| **ABE8e** | dLbCas12a | TTTV V=A,C, G | 4-18 | 23 | Improved PAM applicability (wider range) | - | HEK293T cells | | (59) |
| **ABE8e** | KKH-SaCas9 | NNNRRT | 3-14 (optimal 8-13) | 22 | Reduced size, Improved PAM applicability | Single vector system using AAV8 (60) | HEK293T cells | Mouse (60) | (59) |
| **ABEmax** | SpRYCas9 | NRN>NYN | ~3-9 | 20 | PAM-less | - | HEK293T cells | | (61) |
| **ABE8e** | SpRYCas9 | NRN>NYN | ~3-11 | 20 | PAM-less | - | HEK293T cells, HeLa cells | | (62) |
| **ABE8e-WQ** | SpCas9 | NGG | 4-8* | 20 | Reduced cytosine activity, reduced RNA off-target editing | - | HEK293T cells | | (63) |
| **TaC9ABE** | SpCas9 | NGG | 5-6 (6bp spacer) | 20 | 'Eliminate' Cas9 dependent off target editing | - | HEK293T, HeLa & U2OS cells | | (64) |
| **ABE8e** | Nme2Cas9 | NNNNCC | 2-19 (optimal 6-17) | 24 | Reduced size | Single vector system using AAV9 (65) | HEK293T cells, N2A cells | Mouse (65) | (60) |
| **ABE8e** | SauriCas9 | NNGG | 3-16 | 21 | Reduced size | Single vector system using AAV8 | HEK293T cells, N2A cells | Mouse | (60) |
| **ABE8e** | CjCas9 | NNNVRYAC | 2-18 (optimal 3-15) | 23 | Reduced size | Single vector system, no AAV specified (66) | HEK293T cells, N2A cells | Mouse (66) | (60) |
| **ABE9** | SpCas9 | NGG | 5-6 | 20 | Reduced editing window, reduced bystander editing | RNA mixture injected into zygote | HEK293T cells, HeLa cells | Rodents | (67) |
| **ABE8e-V106W** | denLbCas12a | NTTN, TYCN, TRTV | 8-12 | 23 | Improved PAM applicability, Improved efficiency, reduced off target effects | - | HEK293T cells | | (68) |
| **ABE8e (monomer)** | d12f (nuclease deactivated Un1Cas12f1) | TTTR | N**- 2-4 DS***- 4-6 CL****- complex window | 20 | Improved PAM applicability, reduced size, relatively modest efficiency | - | HEK293T cells | | (69) |
| **ABE8.17** | SpRYCas9 | NRN>NYN | 3-8 | 20 | LMNA context incorporated, improved efficiency, PAM-less. | RNA mixture injected into zygote | | Mouse /Rabbit embryo's, Rabbit | (70) |
| **ABE8.17-NL** | SpCas9 | NGG | 2-4 | 20 | LMNA context incorporated, improved specificity. | RNA mixture injected into embryo | | Rabbit | (70) |
| **ABE8e** | eNme2-T.1 Cas9 | NNNNTN | 7-12 | 23/24 | Improved PAM applicability, at comparable or improved efficiency and off-target effects to SpRYCas9 | Not tested *in vivo* here, should fit in an AAV | HEK293T, HUH7, and U2OS cells | | (71) |
| **ABE8e** | eNme2-T.2 Cas9 | NNNNTN | 7-12 | 23 | Improved PAM applicability, at comparable or improved efficiency and off-target effects to SpRYCas9 | Not tested *in vivo* here, should fit in an AAV | HEK293T, HUH7, and U2OS cells | | (71) |
| **ABE8e** | eNme2-C Cas9 | NNNNCN | 9-16 | 23/24 | Improved PAM applicability, at comparable or improved efficiency and off-target effects to SpRYCas9 | Not tested *in vivo* here, should fit in an AAV | HEK293T, HUH7, and U2OS cells | | (71) |
| **ABE8e** | Nme2Cas9 (i1) | NNNNCN | 1-17 | 24 | Improved PAM applicability, improved activity, reduced size | Single vector system using AAV9 | N2A cells, HEK293T cells, | Mouse | (72) |
| **miniA BE-GG** | SpCas9-NGa | NG | 4-8 | 20 | Increasing precision: high on target editing, lower off target | Split intein dual-AAV system, using AAV9 | HEK293T cells, N2A cells | Mouse | (73) |
| **ABE8e** | SpGCas9 | NGN | 4-8 | 20 | Improved PAM applicability | Split intein dual AAV-system, using AAV9 | HEK293T cells | Mouse | (74,75) |

**Table 1 - *Overview of adenine base editor properties.***
Extensive analysis on adenine base editors and their properties. This includes descriptive properties, such as the enzymatic effector (deaminase) and CRISPR associated protein (Cas-) component of these editors, as well as the preferred protospacer adjacent motif (PAM) sequence, editing window, and protospacer length. Additionally, the optimalizations of the base editor in comparison to SpCas9-ABE7.10 are mentioned, as well as whether the packaging of the editor in Adeno-associated virus (AAV) vectors was achieved. Lastly, the model the editor was studied in, whether that be *in vitro* or *in vivo*, was described.
* Editing window deduced from provided figure; ** N-terminal docking of ABE8e monomer; *** internal docking site ABE8e monomer; **** C-terminal docking of ABE8e monomer.

# Results

## An in-depth literature evaluation revealed 32 possible base editor constructs with advantageous features

In preparation for the selection of the base editors, we performed an extensive literature analysis compiling and comparing data to aid in the prediction of safety, efficiency, and applicability of these editors, in our study (Table 1). Several different factors impact these traits.
To start, we were interested in the protospacer adjacent motif (PAM) sequence of each base editor. The PAM is a conserved sequence, the presence of which is required in the genetic context adjacent to the intended protospacer, to enable hybridization. This motif is located at the 3' end of the protospacer (often positions 21-24). The PAM sequence is dictated and unique to each Cas enzyme. The restrictions imposed by the PAM sequence impact the applicability of the base editor to the genetic context of interest (76). This poses a problem for hard to target genetic loci, that do not contain specific PAM sequences. As a potential solution to this problem, Cas enzymes with increasing flexibility in PAM compatibility were designed. This includes the genetically engineered SpRYCas9 enzyme in particular, as base editors carrying this enzyme are virtually PAM-less. They accommodate both NRN and NYN PAMs, although the NRN PAMs seem to lead to more efficient editing (61).

Another feature, essential for the base editor's efficiency and safety, is the editing window. This is the range within the protospacer in which the deaminase can modify bases. Within the genetic context of interest, the requirement for this window is, that it is wide enough to contain the mutation, in case of a restrictive PAM. Optimally, the mutation is positioned at the site in the active window with the highest editing efficiency. Additionally, the editing window must be narrow enough, to avoid the introduction of bystander edits in adjacent adenines (46). An example of a deaminase that has been engineered to contain a narrow editing window, is ABE9. This deaminase has an editing window spanning from position 5 to 6 in the protospacer, while upholding an average editing efficiency of ~75% at position 5, and ~65% at position 6 (67).

An additional characteristic that is relevant in the search for an appropriate base editor, is the protospacer length. As the editing window is annotated in reference to the first nucleotide in the protospacer, and the PAM sequence encompasses the last few nucleotides in the protospacer, a longer protospacer length increases the distance between the PAM and the active window. This influences the applicability of the editor in the genetic context of interest, give the requirement that the editing window contains the mutation (46). Overall, this length seems to be ~20 bases long, with exceptions up to around 24 bases (Table 1).

Moreover, the specific optimizations attributed to the base editors, as noted in Table 1, are included in our analysis. Every time a new base editor was developed, a feature of that editor was preferrable to their predecessor. First, reducing the size of the base editor constructs is a key optimization. This reduction in size will in time lead to a more effective delivery of base editors, for instance by increasing the likelihood that the editor meets the size requirement for certain single-vector delivery systems. This reduction in size can be achieved by swapping out the traditional SpCas9 enzyme with a smaller Cas9 variant, such as SauriCas9(60). In addition, the size can be reduced by replacing the standard dimer TadA deaminase with a monomer TadA deaminase such as with the 'SECURE-ABEs', which therefore fall under the category of 'miniABE's'(58).
Second, an optimization that has been implemented in newly developed base editors is the narrowing of the editing window in an attempt to eliminate bystander editing. In addition to the ABE9 deaminase mentioned prior (67), other examples are TaC9ABE (A5-A6; specifically, with a 6bp spacer) (64) and ABE8.17-NL (A2-A4) deaminases (70).

Third, the PAM applicability of Cas enzymes is another feature that has been improved upon. Partly by swapping out the traditional SpCas9 (PAM: NGG) (47) with other Cas orthologs such as the pyrimidine-rich-PAM targeting Nme2Cas9 enzyme (PAM: $N_4CC$)(60), and partly by genetically engineering existing Cas enzymes to accept a wider range of PAM sequences, such as in the case of SpRYCas9(61) or KKH-SaCas9(52).
Fourth, an essential feature of a base editor is the efficiency in editing the target nucleotide. This indicates the number of copies of a gene in a sample, that are effectively modified. Which could in turn give an estimation of the fraction of cells in the sample in which the mutation was effectively restored. ABEmax (54) and ABE8e deaminases are examples of deaminases with increasing on-target editing efficiency (59).
Lastly, an optimization that was applied to a number of editors, is the reduction of off-target editing. Off target base editing can be defined as the deamination of nucleotides outside of the loci of interest. This can be harmful as it could potentially introduce mutations (46). This can include RNA off-target editing, which is significantly reduced in ABE8e-WQ (63) and Cas9 dependent off-target editing, which is reduced in TAC9ABE(64).

In later stages of our research, the most efficient editor identified *in vitro* will be evaluated for its efficacy and safety *in vivo*. This is necessary, to determine the impact of the rate of delivery to the heart, and to analyse potential off-target effects. To target delivery of the constructs to the heart specifically, the base editors need to meet the requirements for targeted vector-mediated delivery to the necessary cells and tissues in the animal model (60). Currently, adeno-associated-virus (AAV) vectors are frequently used for the *in vivo* delivery of gene therapy elements to the heart. This gene delivery method is preferred over other viral and non-viral delivery methods, due to multiple factors. Overall, viral vectors are superior to non-viral vectors in their transduction efficiency, and long-term transgene expression (77–79). Within the group of possible viral vectors, AAVs stand out through their ability to transduce non-dividing cells such as cardiomyocytes, and their low immunogenicity (80–82). Moreover, they pose a low risk of insertional mutagenesis, given their expression from episomes (83). The availability of serotypes with cardiac-specific tropism, and cardiac specific promotors, further improves efficiency and prevents the unintended delivery to, and expression in, other organs (84–86). However, AAVs are limited in the size of the construct that they can express (~4.7kb), leading to the inability of certain base editors to meet the size requirements necessary for single-AAV-mediated delivery(77). To include this restriction in our analysis, we registered for each editor whether it had been tested *in vivo*, and whether AAV's were used to deliver the editor to the target tissue. Among the base editors that were tested *in vivo*, three different methods of delivery were reported.
First, the size-optimized editors such as editors carrying SauriCas9, Nme2Cas9, and CjCas9, met the size requirements, and the packaging of these editors in single-vector-AAV systems was tested (60).
Second, other editors such as SpCas9-ABE9 were tested *in vivo*, however this was originally accomplished through the injection of an RNA mixture (mRNA of the construct with sgRNA) into the zygote of the animal model, and the delivery was therefore not targeted to a specific tissue(67).
Lastly, for some larger constructs, a split-intein dual-AAV system was used. This system allows a base editor that does not meet the size requirements for single-AAV delivery, to be delivered to a tissue in two components: a C-terminal section, and an N-terminal section. These sections both contain an intein and are delivered in separate AAV particles. After translation, inteins are removed and the protein segments are reattached to form a full functioning editor. Both SpCas9-NGa- miniABE(GG)(73) and SpG-Cas9-ABE8e have been tested *in vivo* using this system (74).

In addition to this literature-based selection, we decided to add another base editor combination to the list. Namely, SpRYCas9-ABE9. To our knowledge, an analysis on this specific construct has not been published yet. However, given the favourable properties of both the SpRYCas9 variant

(near-limitless PAM applicability), and the ABE9 deaminase (minimal bystander editing), along with the fact that this construct had already been developed within our lab, we decided to include it in our analysis. The PAM sequence was deduced to be the same as other SpRYCas9 carrying constructs, and the editing window was assumed to be the same as other ABE9 deaminase carrying constructs (61,67).

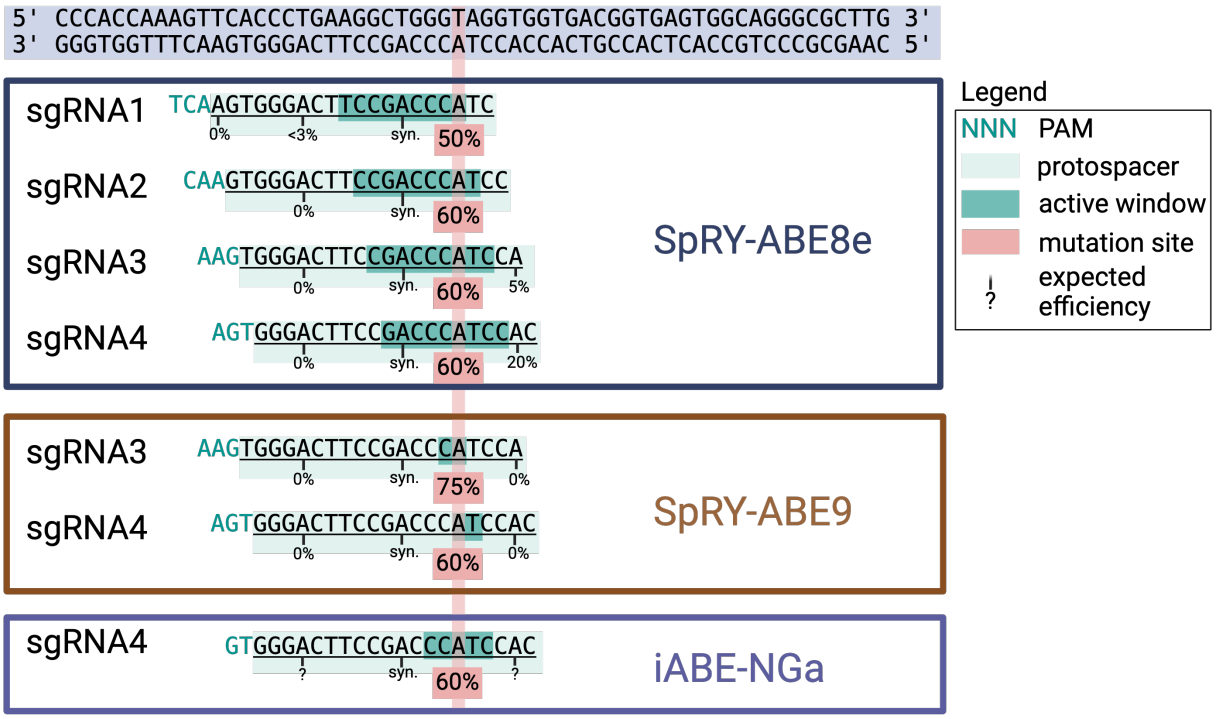


***Figure 2 - overview single guide RNA design.***
The sequence for 'sgRNA3' and 'sgRNA4' were applicable to multiple base editor constructs. Annotated are the percentages representing the expected editing efficiencies of the editor at that site in the protospacer. The efficiencies were quantified in mammalian cell lines (HEK293T for SpRYCas9-ABE8e and SpRYCas9-ABE9 and N2A for iABE-NGa). A smaller chance of bystander edits is indicated by lower percentages for the adenines in the protospacer apart from the mutation site. Higher on-target editing efficiency is indicated by higher percentages at the mutation site adenine. This range of guides was selected based on high on-target and low bystander editing rates compared to other applicable guides.

## Base editors SpRY-ABE9, SpRY-ABE8e and iABE-NGa are most compatible with the genetic context containing the LMNA-Q493X mutation

Upon completion of the literature overview, we proceeded to the design of appropriate single guide RNA molecules to target the mutation of interest (LMNA-Q493X). Optimal guide RNA properties are necessary to properly target a gene locus and position the base editor over the region of interest (46). During this process, all guides were designed by first selecting an appropriate PAM sequence and lining out the protospacer. Then, the active window was highlighted and predicted editing efficiencies were annotated for each adenine in the protospacer.

During the process of guide design, a feature to consider is the aforementioned PAM applicability. If a base editor is compatible with a PAM that is not present in the genetic context, the base editor cannot properly hybridize to the target locus and is therefore removed from further analyses. Given that there is no NGG-PAM located in the sequence adjacent to the possible protospacers,

all base editors that are limited to an NGG-PAM were removed (Table 1). Editors carrying CjCas9 or Nme2Cas9 enzymes, and both base editors denLbCas12a-ABE8e-V106W and d12f (nuclease deactivated Un1Cas12f1)- ABE8e (monomer) were additionally removed due to lacking PAM applicability.

Another feature, essential for proper guide design, is the predicted editing efficiency of the adenines within the protospacer. This includes both the target adenine, as well as other non-synonymous adenines in the protospacer. Adenines that, when modified, result in a synonymous mutation were not considered as they do not induce an amino acid change in the protein, and are not predicted to affect splicing. The aim is a high on-target editing efficiency and low or negligible editing efficiency of other adenines. This ensures effective editing of the target, without inducing bystander edits (46). The thresholds we adhered to, were an on-target editing efficiency of >50%, and a bystander editing efficiency of <20%.

Based on that requirement, a number of possible base editors is not applicable in this genetic context. KKH-SaCas9-ABE7.10, SaCas9-ABE8e, KKH-SaCas9-ABE8e, SauriCas9-ABE8e and SpRYCas9-ABE8.17 are removed based on the high chance of bystander edits (51,59,60,70). SpRYCas9-ABEmax is removed based on its low on-target editing efficiency (61). Guides applicable to dLbCas12a-ABE8e and Nme2Cas9 (i1) (domain in-laid 1) are removed based on both those features (59,72). Furthermore, xCas9-ABE7.10, VQR-Cas9-ABE7.10, and SpGCas9-ABE8e are eliminated based on the fact that there is missing data on their editing efficiency, at the specific sites in the protospacer that house an adenine in our genetic context. In the original analysis, several sites were selected to analyse, and it so happens that the sites that we are interested in, were not analysed(50,53,74). Lastly, exCas9-ABEmax was removed because the editing window of this editor is poorly defined (55).

Regarding the eNme2's (eNme2-T.1Cas9-ABE8e/ eNme2-T.2Cas9-ABE8e/eNme2-CCas9-ABE8e), the constructs were included as potential treatment options *in vitro* due to their PAM applicability, moderately defined editing efficiencies, and their eligibility to be delivered in single-AAV vectors. However, these constructs ultimately did not result in a treatment option to be tested *in vitro*, owing to challenges in the molecular cloning process (71).

After filtering out the ineligible base editor constructs and guides, we are left with seven treatment options to analyse *in vitro*. This includes SpRYCas9-ABE8e with four accompanying sgRNAs, SpRYCas9-ABE9 with two different sgRNAs and miniABE-SpCas9-NGa (henceforth referred to as iABE-NGa) with one sgRNA. All of the mentioned guides were selected based on high on-target and low bystander editing rates compared to other sgRNAs (Fig. 2).
All three of the listed constructs will be used in a split-intein system, to allow for dual-AAV delivery *in vivo*, in later stages of this research. Despite the fact that for the guide associated with iABE-NGa, two non-synonymous adenines in the protospacer have undefined editing efficiencies, we still decided to include them in the analysis. In part because the trend in editing rates seen with this construct moved towards 0% for sites above A11 (73), and in part because pilot studies had been performed in the lab prior to this analysis using this base editor in this genetic context (Fig. 1).

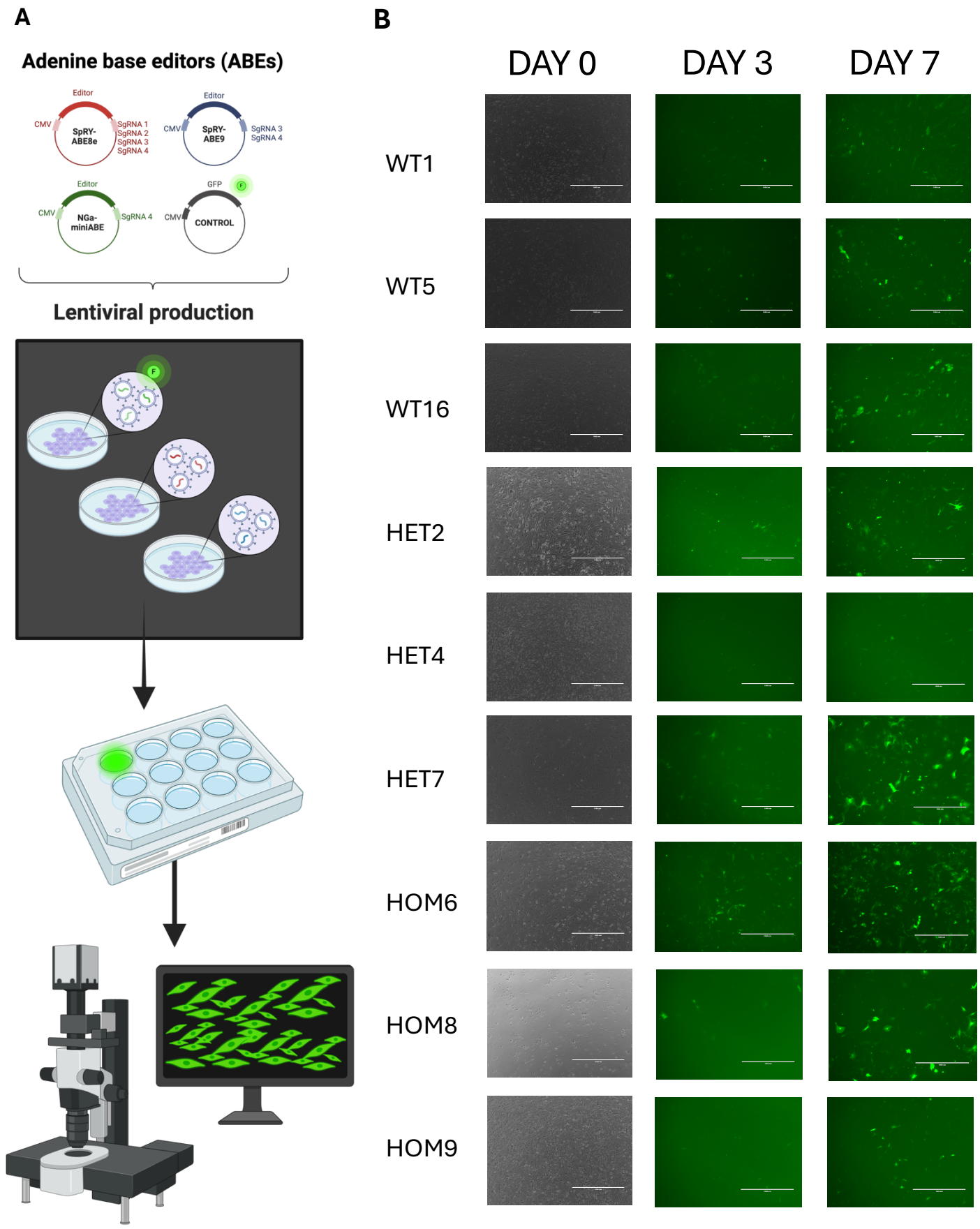


***Figure 3- murine fibroblast transduction with lentiviral base editor treatment.*** A) schematic overview of procedural set-up: One of the lentiviruses produced and used for treatment, contained a GFP reporter. Upon expression this reporter causes a green, fluorescent signal to be emitted from transduced cells. This signal is used to indicate the rate of transduction in a cell line. B) Microscopic images of treated cell lines. For every distinct cell line, images were recorded on the day of treatment (day 0), three days after treatment (day 3) and a week after treatment (day 7). Day 0 images were recorded in the brightfield channel, while day 3 and 7 images were recorded in the GFP fluorescence channel.

## Lentiviral particles carrying the selected base editors transduced murine fibroblasts and led to moderate but heterogenous expression

After selecting the most suitable construct-sgRNA combinations based on a predictive analysis, these combinations were tested *in vitro*. The combinations were packaged into lentiviral particles and used to treat primary murine fibroblasts with either a wildtype ($LMNA^{WT/WT}$), heterozygous mutant ($LMNA^{WT/Q493X}$), or homozygous mutant ($LMNA^{Q493X/Q493X}$) genotype. For every genotype, three biological replicates were used (n=3).

As a reporter for the rate of transduction in each distinct cell line, we included a lentiviral transfer vector expressing green fluorescent protein (pLVX-GFP). One sample per cell line was subjected to the GFP expressing lentivirus. On day 3 and day 7 after transduction, microscopic images were obtained in the GFP channel, to provide an estimate of GFP expression in each cell line. This expression is used as an indication of the rate of transduction in that cell line. An image was additionally taken before transduction, on the same day, to visualize the cell morphology and density prior to the treatment (Fig. 3A).

Overall, the intensity of the signal emitted by this GFP reporter protein, increases from the 3-day timepoint to the 7-day timepoint (Fig. 3B, Fig S3). This could either be a result GFP accumulation over time, or of the increased transduction of cells through prolonged exposure to the treatment. Additionally, certain cell lines portray a more intense expression of GFP, than others. Seemingly, this coincides with cell lines that show a moderate-to-low cell-density (HET7; HOM6; HOM8). Cell lines with seemingly more dense cell diffusion (WT1; HET4; HOM9) seem to also express lower levels of GFP (Fig. 3B, Fig S3).

## SpRYCas9-ABE9 with sgRNA 3 restores the *LMNA/C* mRNA levels in primary murine fibroblasts most consistently

To investigate the efficiency with which the selected base editors contribute to the restoration of *LMNA/C* expression, primary murine fibroblasts of wildtype ($LMNA^{WT/WT}$), heterozygous mutant ($LMNA^{WT/Q493X}$), or homozygous mutant ($LMNA^{Q493X/Q493X}$) mice were treated with one of the seven previously described treatment options (1000 viral genomes/cell). After seven days of exposure to these treatments the RNA was isolated from the 108 different samples and subjected to quantitative polymerase chain reaction analysis for *LMNA/C*, *LMNA* specific, and *LMNC* specific mRNA levels (Fig. 4A).

As expected, *LMNA/C* mRNA levels, as well as *LMNA* and *LMNC* specific mRNA levels are significantly reduced in the heterozygous cell lines, and further reduced in the homozygous cell lines, when left untreated (Fig. 4). This remains true for every experimental condition. On average, heterozygous samples show a decrease in *LMNA/C* expression levels of approximately 50%, and homozygous samples show a ~85% decrease. *LMNA* specific levels show a ~61% decrease in heterozygous samples and a ~91% decrease in homozygous samples. Lastly, *LMNC* specific expression shows an average reduction of ~51% in heterozygous samples, and ~70% in homozygous samples.

Additionally, a restoration of *LMNA/C* mRNA levels is seen in certain experimental conditions. In Heterozygous samples, SpRY-ABE8e with sgRNA3 (8e.3) shows the largest increase in *LMNA/C* mRNA levels, improving them with ~56% from the untreated baseline. Other treatment options that showed a sizable increase in *LMNA/C* expression, are SpRY-ABE9 with sgRNA3 or sgRNA 4 (9.3/9.4), which respectively increased them by ~40% and ~41% (Fig. 4B/E). In homozygous samples, editor combination 9.3 shows the greatest restoration of *LMNA/C* levels, increasing them ~116% from the untreated baseline (Fig. 4B/F).

Along with *LMNA/C* total mRNA levels, *LMNA* specific mRNA levels also show an increase in certain experimental conditions. This specifically entails homozygous samples. Both SpRY-ABE8e with sgRNA 1 (8e.1) and 9.3 show the largest increase of *LMNA* specific expression levels in homozygous samples, leading to a respective ~78% and ~96% increase of *LMNA* mRNA levels compared to untreated baseline levels (Fig. 4C). Regarding *LMNC* specific expression, treatment 9.3 results in the largest increase, with a ~133% increase in heterozygous samples, and a 144% increase in homozygous samples compared to

untreated controls (Fig. 4D). In conclusion, the combination SpRYCas9-ABE9 with sgRNA shows the most consistent restoration of LMNA/C, LMNA and LMNC transcript levels.

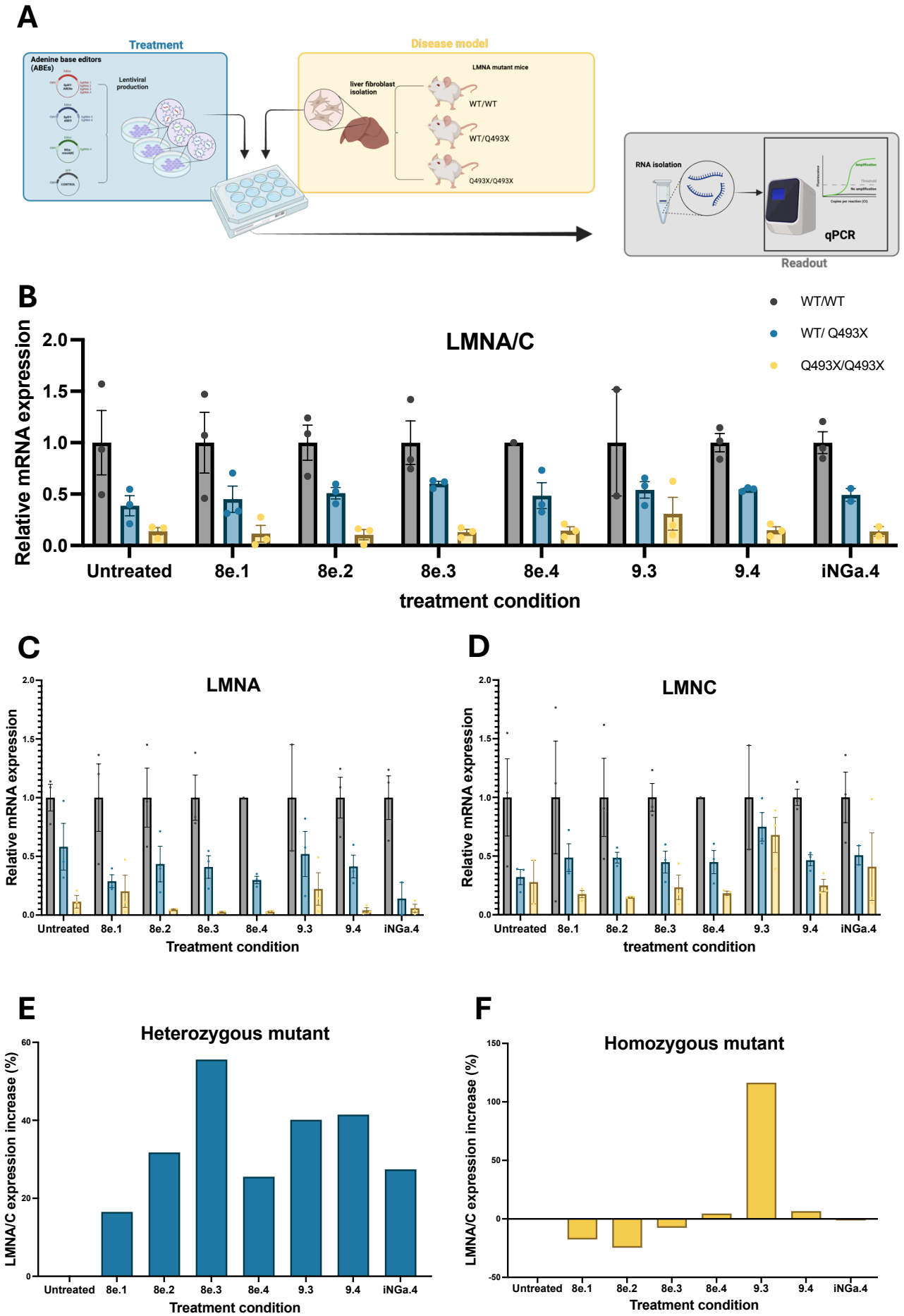
A
Treatment
Adenine base editors (ABEs)
Lentiviral production
Disease model
LMNA mutant mice
liver fibroblast isolation
WT/WT
WT/Q493X
Q493X/Q493X
RNA isolation
qPCR
Readout
B
LMNA/C
WT/WT
WT/ Q493X
Q493X/Q493X
Relative mRNA expression
2.0
1.5
1.0
0.5
0.0
Untreated
8e.1
8e.2
8e.3
8e.4
9.3
9.4
iNGa.4
treatment condition
C
LMNA
Relative mRNA expression
Treatment condition
D
LMNC
Relative mRNA expression
treatment condition
E
Heterozygous mutant
LMNA/C expression increase (%)
60
40
20
0
Treatment condition
F
Homozygous mutant
LMNA/C expression increase (%)
150
100
50
0
-50
Treatment condition

***Figure 4 there is a trend in LMNA/C total and LMNC levels that favours base editor combination SpRY-ABE9+sgRNA3 in this analysis.*** **A)** Schematic overview of experimental setup. Primary fibroblast isolated from wildtype (WT/WT), heterozygous (WT/Q493X) or homozygous (Q493X/Q493X) mutant mice were treated with lentivirus particles containing one of the base editor treatments. RNA was isolated from these samples and subjected to quantitative polymerase chain reaction analysis. **B)** Quantitative polymerase chain reaction (qPCR) data of LMNA/C total mRNA levels in WT/WT, WT/Q493X and Q493X/Q493X mutant mouse fibroblast samples treated with one of the base editor treatments: pLVX-SpRY-ABE8e+ sgRNA 1, 2, 3, or 4 (8e.1, 8e.2, 8e.3, 8e.4), pLVX-SpRY-ABE9+ sgRNA 3 or 4 (9.3, 9.4), pLVX-iABE-NGa +sgRNA 4 (iNGa.4). All WT/Q493X and Q493X/Q493X measurements in this figure are normalized to the wildtype sample under the same condition. Values and error bars indicate mean +/- s.e.m. Significance for comparison was analyzed with two-way analysis of variance (ANOVA) where Genotype factor has a significance of ****P<0,0001, both treatment factor and interaction between factors is non-significant (ns.) (n=3) **C)** qPCR analysis of LMNA specific mRNA levels in WT/WT, WT/Q493X and Q493X/Q493X mutant mouse fibroblast samples under one of the selected treatment conditions. Values and error bars indicate mean +/- s.e.m. significance for comparison was analyzed with two-way analysis of variance (ANOVA) where Genotype factor has a significance of ****P<0,0001, both treatment factor and interaction between factors is non-significant (n=3) **D)** qPCR analysis of LMNC specific mRNA levels in WT/WT, WT/Q493X and Q493X/Q493X mutant mouse fibroblast samples under one of the selected treatment conditions. Data are mean +/- s.e.m. Significance for comparison was analyzed with two-way analysis of variance (ANOVA) where Genotype factor has a significance of ****P<0,0001, both treatment factor and interaction between factors is non-significant (n=3) **E)** Percentual increase of LMNA/C mRNA levels in heterozygous mutant samples in comparison to the untreated heterozygous sample (ns.). **F)** Percentual increase of LMNA/C mRNA levels in homozygous mutant samples in comparison to the untreated homozygous sample (ns.).

## Discussion

Cardiac laminopathies affect up to 8% of patients with familiar DCM, making it one of the most prominent causes of familiar DCM (3). Additionally, these mutations contribute to full penetrance from the age of 60, thereby eventually affecting every individual carrying them (1). Patients with LMNA-DCM additionally face a higher rate of mortality, transplantation and major cardiac events compared to DCM patients with other mutations (5). Aside from a limited number of symptomatic treatments, there is no cure available for patients suffering from this disease (4,34,35). Gene therapy could provide a potential path for curative treatment options. However, data on these approaches is limited within this disease context.

Studies investigating these approaches are not comprehensive enough to warrant considerable treatment options in humans. The study conducted by Salvarani et al. for instance, reported the correction of the cardiac specific LMNA-K219T mutation in hiPSC derived cardiomyocytes. Instead of an administered treatment however, the correction was achieved through the selection and isolation of a corrected clone. This resulted in a lack of information considering dose-dependency and transduction efficiency of the required vector (38). Another study, conducted by Frock et al. analyzed the potential of LMNA overexpression to enact functional improvement in a LMNA knockout mouse model. This study is limited in its translatability considering the fact that a full knockout has not been reported in a living patient and is likely not compatible with life in humans. Moreover, the functional recovery and extension of lifespan in mice, is described as 'modest' in the paper, indicating a lack of robustness (39). Scharner et al. reported an alternative approach to gene therapy for laminopathies. This study analyzes the potential of exon-skipping to exclude the mutation from the translated transcript. However, little was discussed about the safety of the treatment and potential aspecific oligo binding was not evaluated (40). None of the listed studies included a safety analysis evaluating off-target effects. Some of them, did not incorporate an *in vivo* element to begin with (38–40).

When looking for a curative approach to cardiac laminopathies, it is essential that the safety profile is well defined. When treating already compromised individuals it is imperative that introduction of additional potentially harmful changes in the DNA, or changes in organs other than the target organ, are prevented. There is therefore a need for additional studies that include therapeutic safety in their analysis, along with evaluations on efficiency and functional recovery, before clinical potential can be realized.

Studies including a safety overview have been reported for non-cardiac LMNA mutations before, such as for Hutchinson-Gilford progeria syndrome (HGPS). Liu et al. for instance have reported the efficient correction of HGPS associated LMNA mutations with unobserved genetic and epigenetic abnormalities (87). Additionally, Koblan et al. described efficient base editing of HGPS related mutations along with an off-target DNA and RNA editing analysis to determine safety. Such data considering cardiac laminopathies however, are limited (88). In addition to *in vitro* and *in vivo* experiments, a potential tool to facilitate the evaluation of off-target effects attributable to the different genetic therapies, is a computational analysis to predict these features. This has been applied in the study reported by Yang et al., in which they predicted the safest single guide RNA sequences in the targeting of adenine base editor constructs to edit a LMNA mutation (49).

In this study, we performed a thorough predictive analysis selecting the most suitable and safe base editors to treat a patient-specific LMNA mutation (Q493X), which we subsequently tested *in vitro*. We predicted that within the LMNA-Q493X genetic context, base editors SpRYCas9-ABE8e, SpRYCas9-ABE9 and SpCas9NGa-miniABE-GG (iABE-NGa) would most efficiently modify the mutation, while leaving bystander adenines mostly unedited. We were then able to design four applicable sgRNAs for SpRYCas9-ABE8e, two sgRNAs for SpRYCas9-ABE9 and one for SpCas9NGa-miniABE-GG (Fig. 2). Finally, we found that SpRYCas9-ABE9 with single guide RNA 3 most efficiently and consistently restored the expression levels of both *LMNA* and *LMNC* transcripts in primary murine liver fibroblasts.

Initially, we compiled a selection of 31 different base editors as potential treatment options for this study. Of these constructs, 14 were removed based on lacking PAM applicability in the genetic context of the mutation. SpRYCas9-ABE9 that has not been published yet, was added, based on its availability in the lab, and features of this editor were inferred from separate articles. From the 18 remaining editors, seven more were removed based on unclear or missing data, that was necessary to properly evaluate potential sgRNAs. Finally, eight additional editors were removed from the selection, either due to inefficient on-target editing, a high risk of bystander editing, or both.
The three remaining base editors, SpRYCas9-ABE8e, SpRYCas9-ABE9 and SpCas9NGa-miniABE-GG, were selected for further analysis. First, we used restriction cloning to produce lentiviral transfer plasmids with the selected base editors. We then designed eligible sgRNAs and used restriction cloning to insert them into the respective lentiviral transfer plasmids. We subsequently produced lentiviral particles containing the editors with their guides and used them to treat primary murine liver fibroblasts (Fig. 4).
Upon treatment of murine liver fibroblasts from wildtype ($LMNA^{WT/WT}$), heterozygous mutant ($LMNA^{Q493X/WT}$) or homozygous mutant ($LMNA^{Q493X/Q493X}$) mice, the degree of transduction indicated by GFP reporter expression, was heterogenous. This heterogeneity seems to correlate with cell density (Fig. S3).
Using the samples derived from this 7-day treatment, RNA was isolated for further molecular analysis. Quantitative polymerase chain reaction (qPCR) analysis of *LMNA/C* transcripts showed that overall, the $LMNA^{WT/WT}$, $LMNA^{Q493X/WT}$ and $LMNA^{Q493X/Q493X}$ cell lines were significantly different from each other in *LMNA/C*, *LMNA* and *LMNC* transcript levels (****$p<0.0001$). This is expected, since the LMNA-Q493X mutation causes a haploinsufficiency in the allele carrying the mutation. We expect 50% of the mRNA transcript levels seen in the $LMNA^{WT/WT}$ samples, to be present in $LMNA^{Q493X/WT}$ samples, while we expect no *LMNA/C* mRNA transcript in the $LMNA^{Q493X/Q493X}$ samples. This is reflected in the mRNA levels as seen in figure 4. Similar findings are shown for both *LMNA* and *LMNC* specific mRNA levels.
We compared treated samples with the untreated controls and found no statistically significant differences. However, the data shows a trend supporting the use of SpRYCas9-ABE9 with sgRNA 3. This combination repeatedly resulted in the most effective restoration of *LMNA/C* total, *LMNA* and *LMNC* specific mRNA transcript levels.
It is noteworthy that *LMNA* and *LMNC* mRNA transcript levels do not follow the same pattern of restoration, in the same sample, indicating a possible change in the ratio between *LMNA* and *LMNC* abundance. A similar feature was reported in an earlier study, investigating a distinct nonsense mutation. In this study, Lamin A levels were reduced more severely than Lamin C levels were. This was a consequence of a lower level of the wildtype Lamin A protein (89). Other reports have shown additional shifts in the ratio between Lamin A and C expression, upon disease. This was reported in HGPS by Reunert et. al. and in Emery-Dreifuss muscular dystrophy (EDMD) by Niebroj-Dobosz et. al. (90,91). It is suggested that lower levels of Lamin A influence the stability and resilience of the healthy LMNA allele and its expression (92). It is therefore possible, that diminished Lamin A levels, influence the ability of the isoform to be restored in expression, upon correction of the mutation.

A considerable limitation of this study is the lack of statistical power in our conclusions. The statistical power of experimental results in an analysis of variance (ANOVA) are dependent on, among other factors, sample size, effect size, and error variance (or unexplained variance)(93).
In this study, the variation within the experimental group, or the unexplained variance was large in certain groups, when compared to the variance between sample means.
This could be a result of the fact that the samples used, were derived from primary murine cell cultures, which can be heterogenous in their genetic expression. The heterogeneity in primary cultures can be influenced through three different factors. Firstly, due to technical limitations it is

difficult to accurately obtain a pure population of fibroblasts, from tissue samples. Contaminations of other cell types might cause a shift in the bulk measured expression of certain genes (94). This includes LMNA, as this gene can have cell-type specific expression levels. With the many distinct cell-types present in the liver, expression levels range from 16.9 (in residing T-cells) to 306.5 (in smooth muscle cells) transcripts per million (nTPM) (95). Contaminations with cells especially high or low in *LMNA* expression could therefore influence the bulk expression of *LMNA* in murine fibroblast samples. Next, the donor heterogeneity between mice of the same inbred strain can contribute to the unexplained variance seen between samples in the same experimental group. Though inbred strains are categorically standardized in their genetic information, features such as genetic drift and unique epigenetic patterns can contribute to differences in expression (96,97). Lastly, fibroblasts are cells that react to changing external factors by changing their functional and phenotypic features. Either through signals derived from the cellular microenvironment, or in this case due to cell culture related conditions, adaptations in individual fibroblasts might influence variation in genetic expression and cellular identity (98,99)
In addition to the heterogenous cell model, a contributor to the variation seen in the different samples, could be efficiency of transduction, which was shown to be heterogenous through expression of the GFP reporter (Fig. 3). Previously, Wang et al. showed that moderate cell density is optimal to facilitate gene transfection and that high and low cell density impair it. In future experiments, this variation could be prevented by including a standardization of cell density, such as through the use of micropatterned surfaces to control this feature, prior to treatment. This could homogenize the rate of transduction, and therefore diminish that additional variable (100).

Another feature of this study that potentially leads to the lacking statistical power, is the relatively small sample size. Every experimental group, that both shared the same genotype and the same treatment condition, consisted of three biological replicates. There were no technical replicates available. This can be explained by the fact that murine livers are limited in the cell number that can be derived from them, as they weigh on average 2-3 grams (101). Furthermore, fibroblasts are not the most abundant cell-type in murine livers. Fibrogenic cell types make up less than 8% of the hepatic tissue in healthy mice, explaining the limited yield (102). Primary cell cultures are additionally limited in their proliferation and life span, which would make adequate expansion difficult (103). Considering the number of treatment options we included, more technical replicates were therefore not available per condition. An approach to take to improve this sample size in future endeavors, is to use a cell-source, from which more technical replicates can be derived. An example of such a cell source, is an immortalized cell line which can be grown and expanded for longer (104). Furthermore, instead of using every cell culture well as a singular bulk sample, it is worth looking into single-cell approaches, that vastly increase your sample size, as well as the depth of the data that you derive from the approach. This increase in sample size improves the statistical power (105).

As the aim of this study, was to determine the safest, as well as the most efficient treatment option, it is worth mentioning that in this study the safety of these base editors was not evaluated in an *in vitro* experiment. However, we did use the data available on the properties of the editor constructs to infer the likelihood of harmful effects, due to bystander editing. In following studies, an *in vitro* experiment should be included to quantify editing rates of the target, as well as bystander adenines directly. This can be achieved through amplicon sequencing which is often used to evaluate newly developed base editors for bystander editing (67,106,107). This method facilitates the targeted and sensitive sequencing of a specific genetic locus, using its amplification (108). It might be advantageous to additionally, include an assessment of other types of off-target effects.

The goal of this particular study was not to achieve optimal translatability. The objective was rather, to identify the most effective and safe option *in vitro*. However, in future studies, the potential for translation is an important element to factor in when moving towards clinical practice. To achieve the translation of this treatment approach to the human body, a transition would need to be made into a cardiomyocyte-or at least muscle-specific cell type, as the symptoms related to cardiac laminopathies are mainly focused on these tissues (109). Later, the introduction of *in vivo* studies should be considered, to better analyze the systemic effects connected to delivery and targeting of the cardiac tissue (35). To enhance this, it might be necessary to include size-optimized base editors to the study, that can be packaged in a single-AAV delivery system. This enables the use of lower doses, to achieve similar editing efficiencies (60). Additionally, to target the cardiac cells more efficiently, and prevent off-target effects in other tissues, the use of cardiac-specific promotors, enhancers, or viral vector serotypes might be included. This diminishes the expression of the base editors in non-cardiac tissues, preventing them from exerting their editing effects undesirably (45,84–86).

SpRY-Cas9-ABE9 with sgRNA 3 seemingly is the most efficient base editor combination to restore the reported LMNA-Q493X mutation *in vitro.* Looking back at the predictive analysis (Fig. 2), this exact combination was expected to yield the most efficient on target editing efficiency (~75%) of all the treatment options. Together, these findings provide evidence for the potential of literature-based predictions in the customization of gene editing approaches. Variation between gene editing target-loci poses a challenge in the development of one effective treatment option for all genetic mutations causing the same condition (111). Therefore, the personalization of gene editing approaches can vastly improve the efficiency and safety of these approaches on an individual basis. The use of a literature based predictive analysis to pre-select suitable editors and single guide RNAs, can significantly cut down on the required resources and time needed for this personalization (49). Numerous computational and AI driven tools have been developed to aid in this process. These tools enable scientists to easily design editing approaches, while considering many factors including genetic context and predicted off-target effects. This concept could further facilitate the high-throughput customization of genetic treatments, which is essential in the development of curative therapies to correct all cardiac laminopathies (112–115).
This study, therefore, does not only provide insights into the restoration of haploinsufficiency caused by LMNA-Q493X mutation. It additionally sets a precedent in the use of a selective prediction to streamline the development of new and case-specific gene therapies.

## Supplementary materials

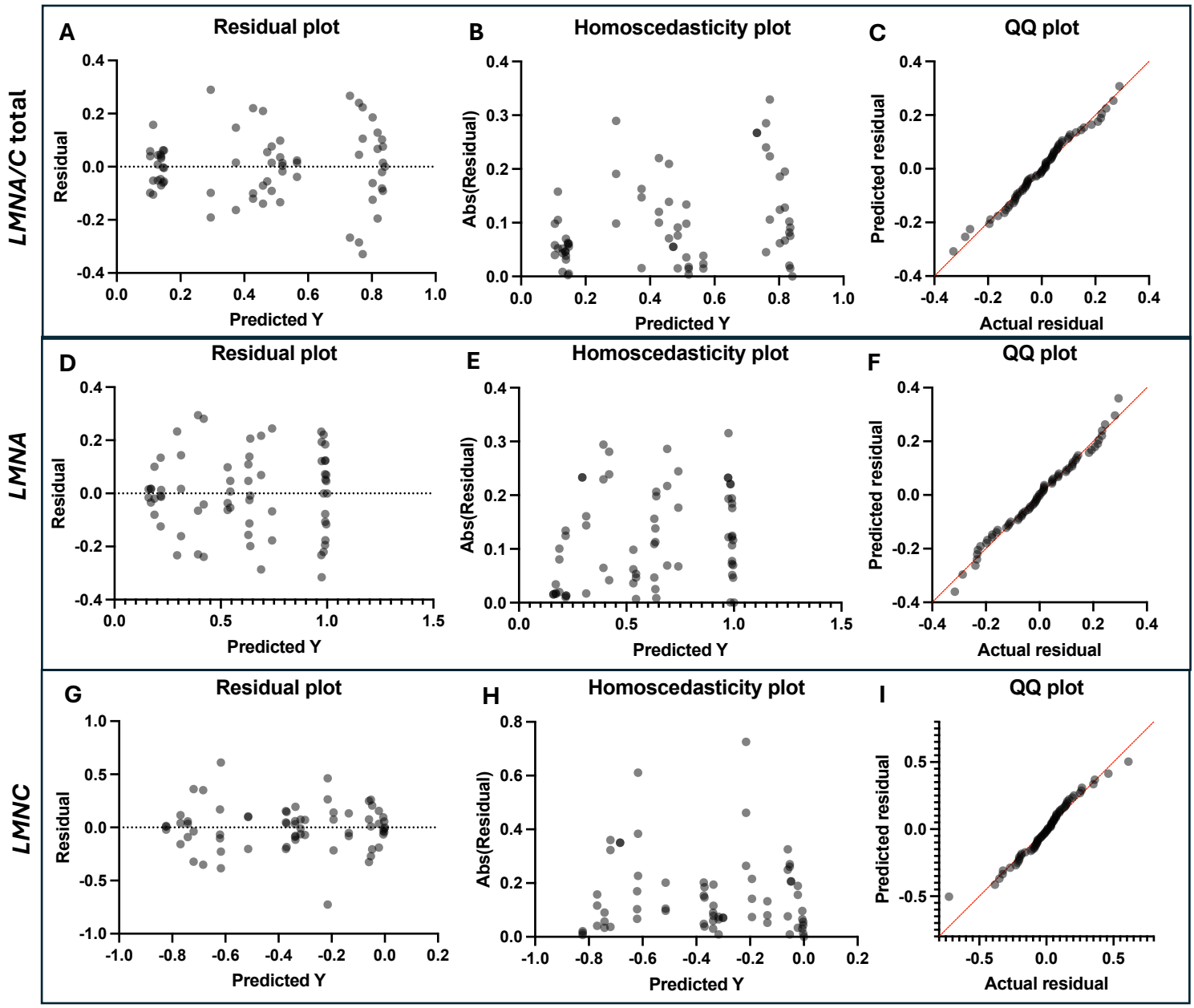


***Figure S1 residual graphs of qPCR data*** A-C) shows plots visualizing both homoscedasticity and normality of the *LMNA/C* total quantitative polymerase chain reaction (qPCR) data. Data were sin(Y) transformed to improve normality and homoscedasticity. Transformed data were used for further statistical analysis. D-F) Residual graphs for *LMNA* qPCR data. Data were √Y transformed. Transformed data were used for further statistical analysis. G-I) Residual graphs for *LMNC* qPCR data. Data were log(Y) transformed. Transformed data were used for further statistical analysis.

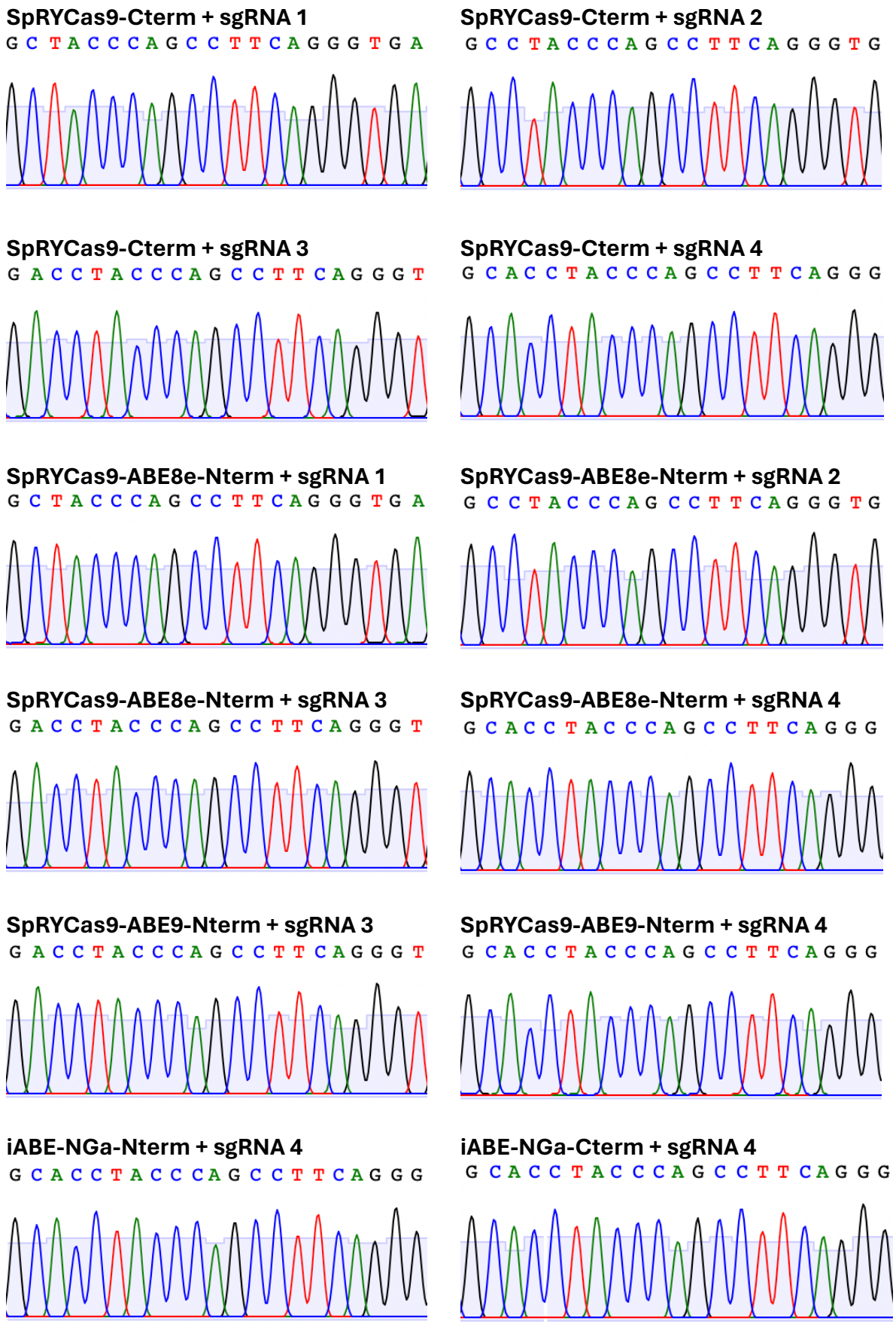


***Figure S2 sequencing data sgRNA cloning.*** Sequence reads confirming sgRNA insertion into base editor plasmids. Reads were obtained through Sanger sequencing using a U6 forward primer.

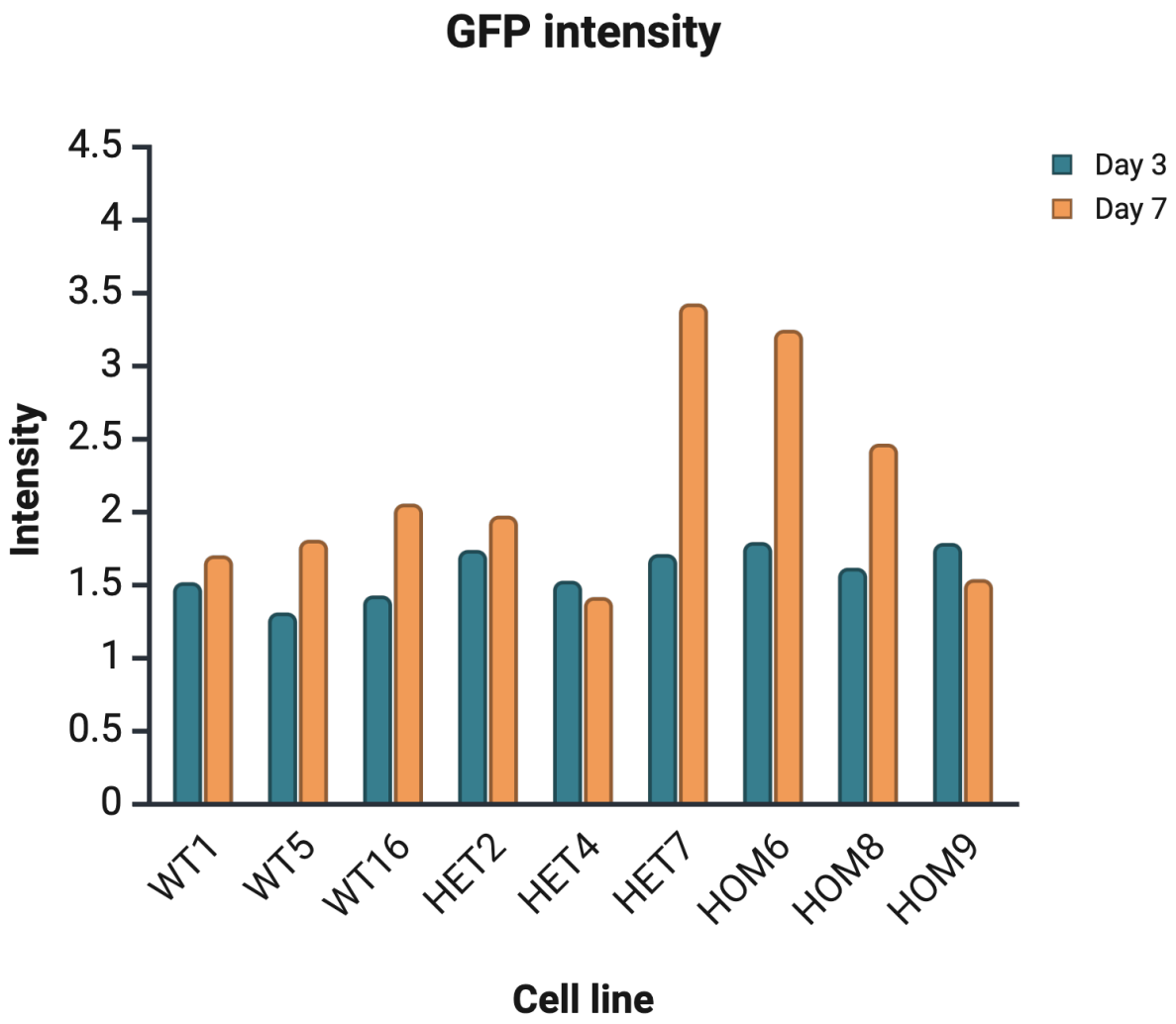


***Figure S3*** *Quantification of GFP intensity captured from individual cell lines on day 3 and 7. The background signal was removed using the rolling ball method in ImageJ prior to measurement of GFP signal in ImageJ.*

## Supp. Table 1. Overhang PCR primers

| PCR-product | Forward primer | Reverse primer |
|---|---|---|
| iABE-Nga Nterm | TCCACCGGTCGACGGAAGC GAGTTCGAGTCACC | AGGCTCGAGGTACCTCCCCAGCATGC CTGCTAT |
| iABE-Nga Cterm | AGGACCGGTGCCTGCTAAAA ATAACCCTGT | AGGCTCGAGGTACCTCCCCAGCATGC CTGCTAT |

## Supp. Table 2. Murine qPCR primers

| qPCR-target | Forward primer | Reverse primer |
|---|---|---|
| *LMNA/C* total | TCGAATCCGCATTGACAGCC | CTCCAGGTCACGCAGCTTTG |
| *LMNA* | GACCCCGCTGAGTACAACCTG | GCGGAAGCTTCGAGTGACTG |
| *LMNC* | CGACGAGGATGGAGAAGAGC | AGACTTTGGCATGGAGGTGG |

## Supp. Table 3. Sanger sequencing primers

***Table S3*** An overview of sequencing primers used to confirm the cloning of base editor constructs, based on alignment to predesigned plasmid maps (appendix 1-5). Fw: Forward primer. Rv: Reverse primer. CMV: cytomegalovirus promotor. U6: U6 promotor. SC: SpRY-Cas9-Cterm. 8e/9: SpRY-Cas9-ABE8e-Nterm/SpRY-Cas9-ABE9-Nterm. iN: iABE-NGa-Nterm. iC: iABE-NGa-Cterm. M: referring to a primer designed in the middle of the construct.

| Sequencing primers | Sequence |
|---|---|
| CMV-Fw | CGCAAATGGGCGGTAGGCGTG |
| U6-Rv | AATCATGGGAAATAGGCCCTC |
| U6-Fw | GAGGGCCTATTTCCCATGATTC |
| SC Rv into CMV | GGTGTATCTCCGCCGCTTCA |
| 8e/9 Rv into CMV | AGTTCAGCACGTTCATCAGGGA |
| iN Rv into CMV | GTGATTCATGCCGGGGTAGTGC |
| iC Rv into CMV | CCACTGACTTCTATGTCTATAAGCT |
| SC Fw M | GCCGGCTTCATCAAGAGACAGCT |
| 8e/9 Fw M | CTGACCCCCAACTTCAAGAGCA |
| iN Fw M | GCCTGTTCGGAAACCTGATTGCC |
| iC Fw M | GCCAGATCCTGAAAGAACACCCCG |
| SC Rv M | GCCTTATCCAGTTCGCTCAGGC |
| 8e/9 Rv M | GTGATCTCGGTGTTCACTCTCAGGAT |
| iN Rv M | CACCAGCTGGATGAACAGCTTGTCCAC |
| iC Rv M | GCTGGGTGTTTTCCACGGGGTGTT |

## Supp. Table 4. Titer determination results

***Table S4*** *Titer determination results of the produced lentiviral treatments expressed in viral genomes per mL.*

| Virus | Concentration (vg/mL) |
|---|---|
| LV-GFP | $6,62*10^8$ |
| LV-SpRY C-term guide 1 | $7,95*10^8$ |
| LV-SpRY C-term guide 2 | $5,92*10^8$ |
| LV-SpRY C-term guide 3 | $7,34*10^8$ |
| LV-SpRY C-term guide 4 | $6,45*10^8$ |
| LV-SpRY ABE8e N-term guide 1 | $8,08*10^8$ |
| LV-SpRY ABE8e N-term guide 2 | $8,79*10^8$ |
| LV-SpRY ABE8e N-term guide 3 | $3,09*10^9$ |
| LV-SpRY ABE8e N-term guide 4 | $1,71*10^9$ |
| LV-SpRY ABE9 N-term guide 3 | $1,67*10^9$ |
| LV-SpRY ABE9 N-term guide 4 | $5,70*10^8$ |

# Appendix 1: #304 706_pAAV_iABE-NGa_CAS9_Cterm

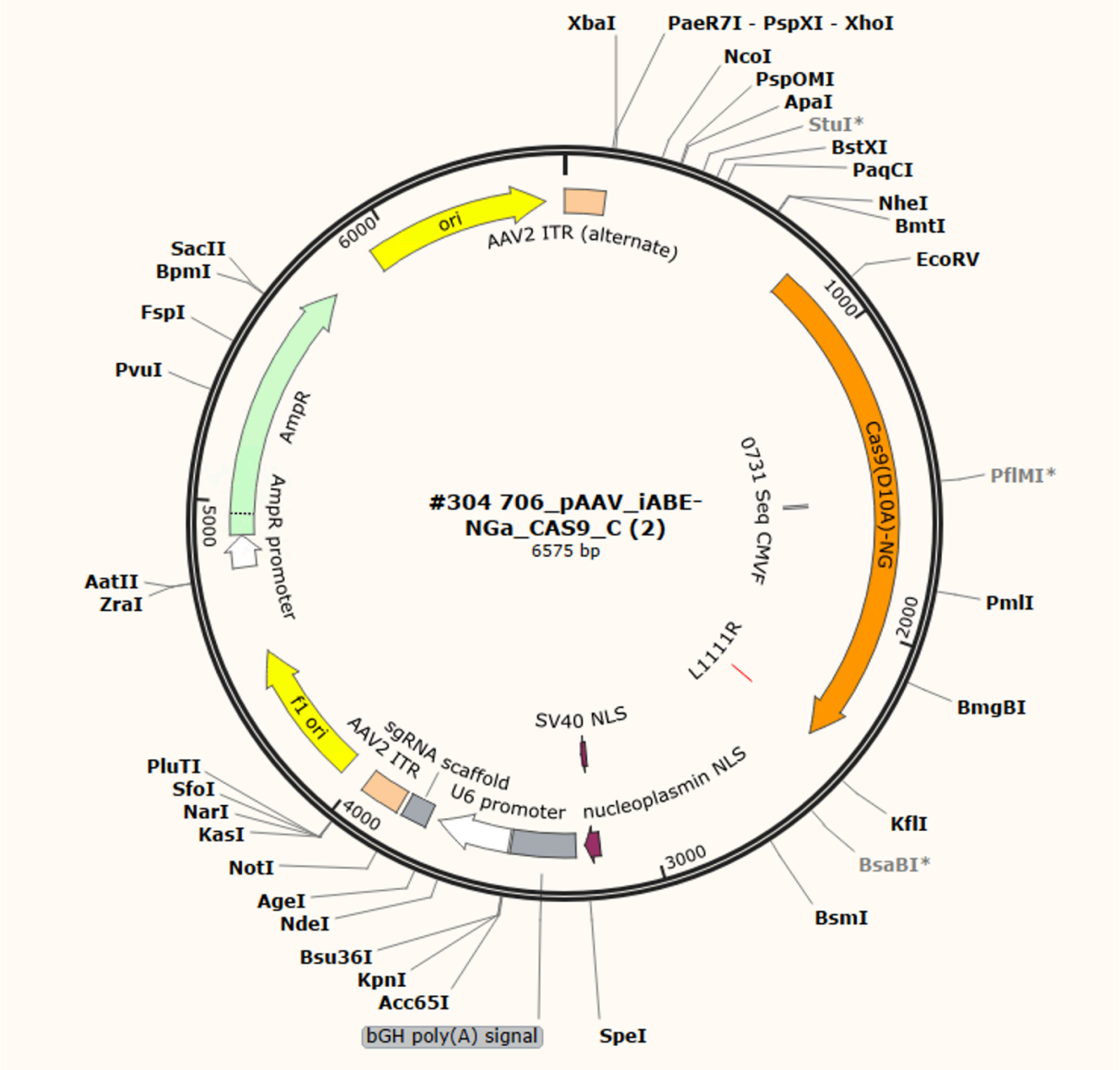

# Appendix 2: #305 855_pAAV_iABE-NGa_CAS9_Nterm

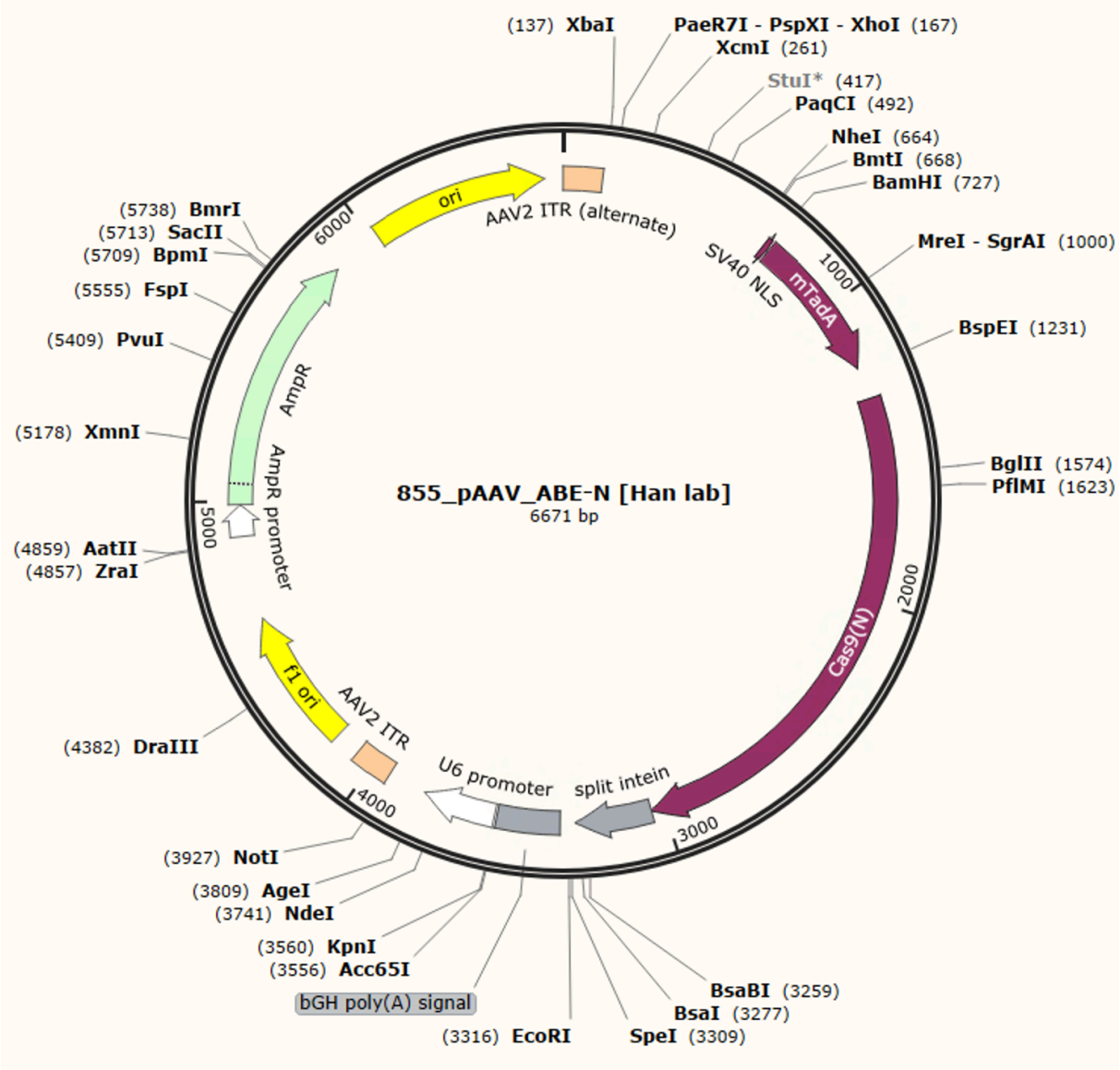

# Appendix 3: SpRY-Cas9-Cterm plasmid map

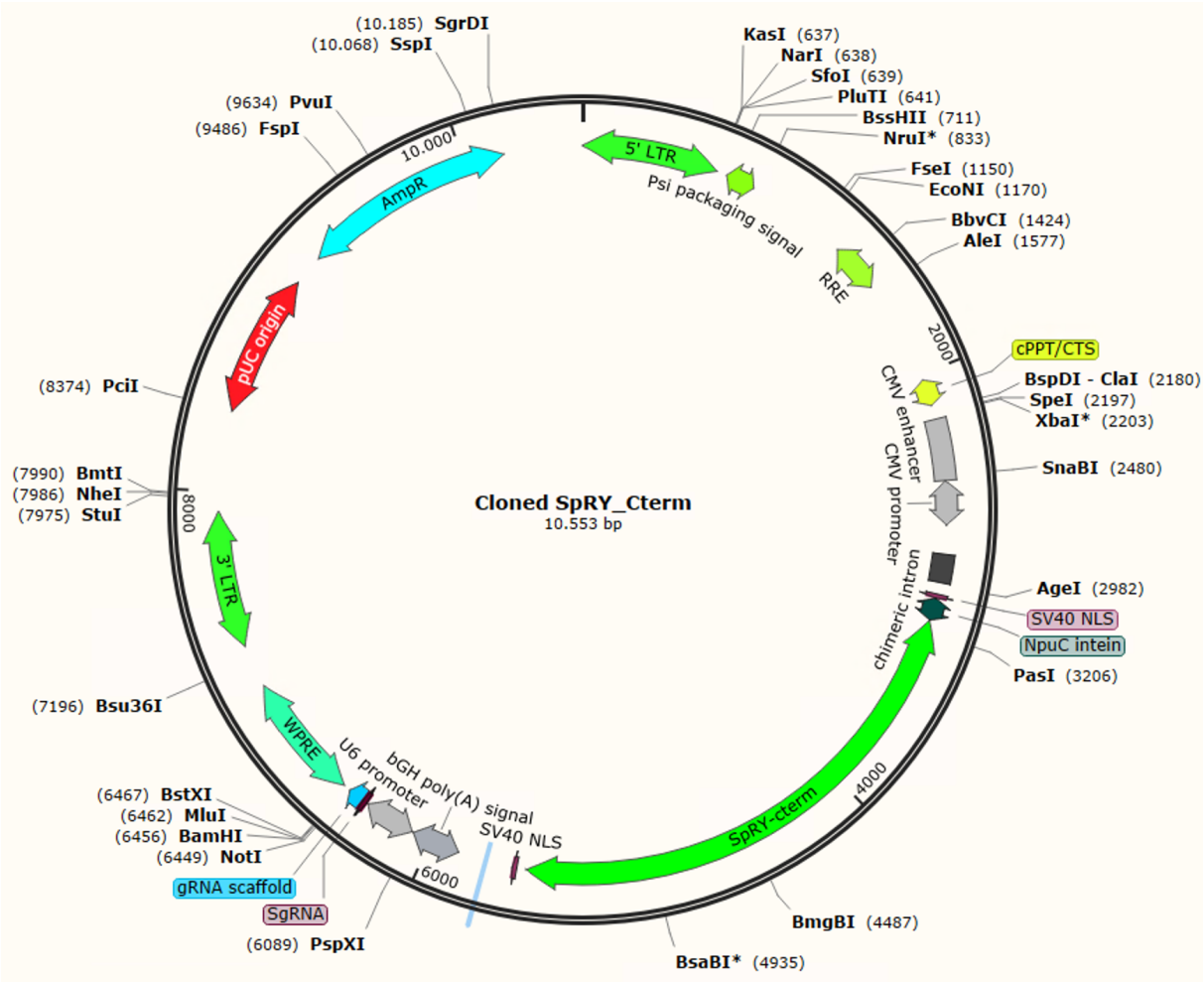

# Appendix 4: SpRY-Cas9-ABE8e-Nterm plasmid map

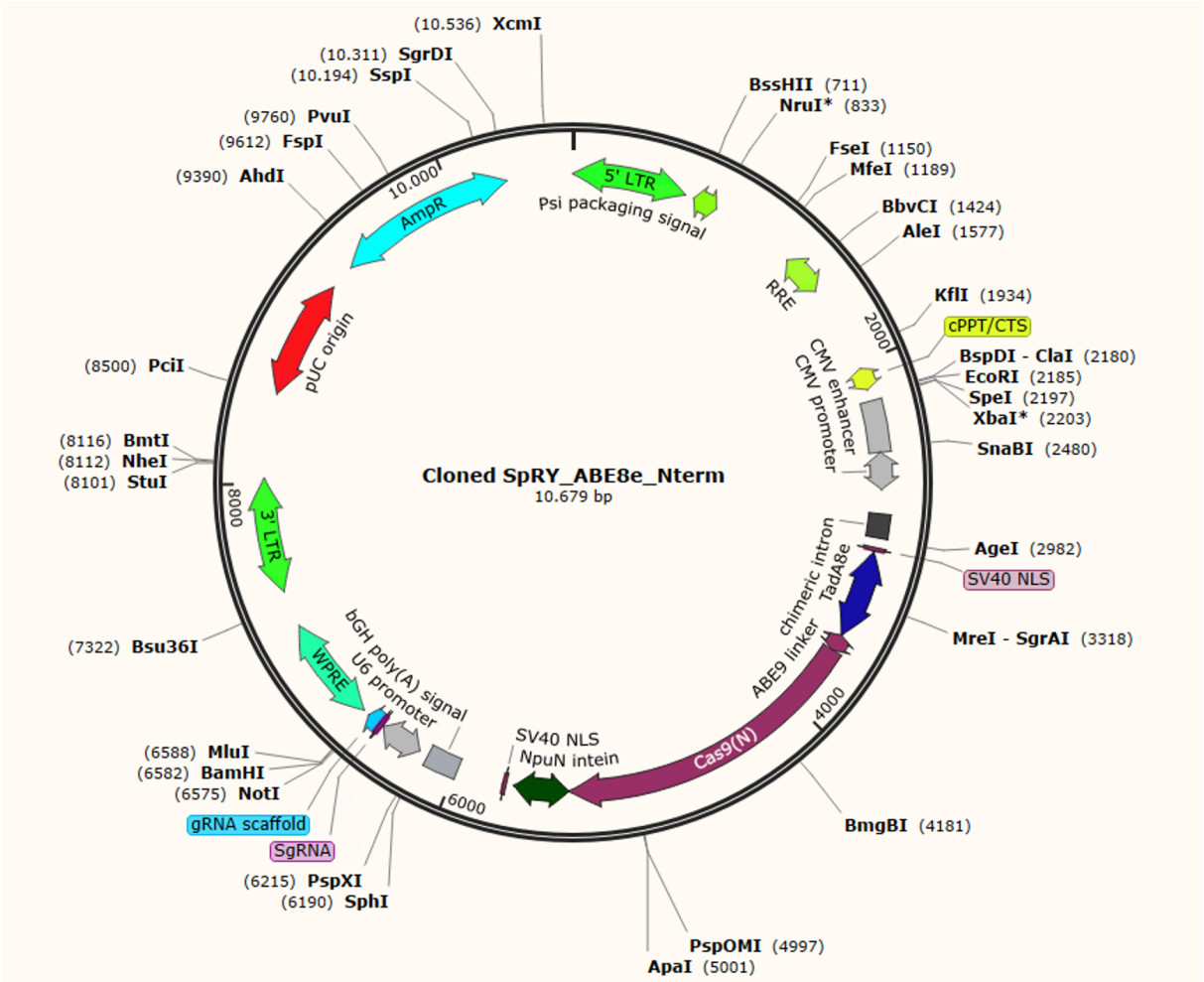

# Appendix 5: SpRY-Cas9-ABE9-Nterm plasmid map

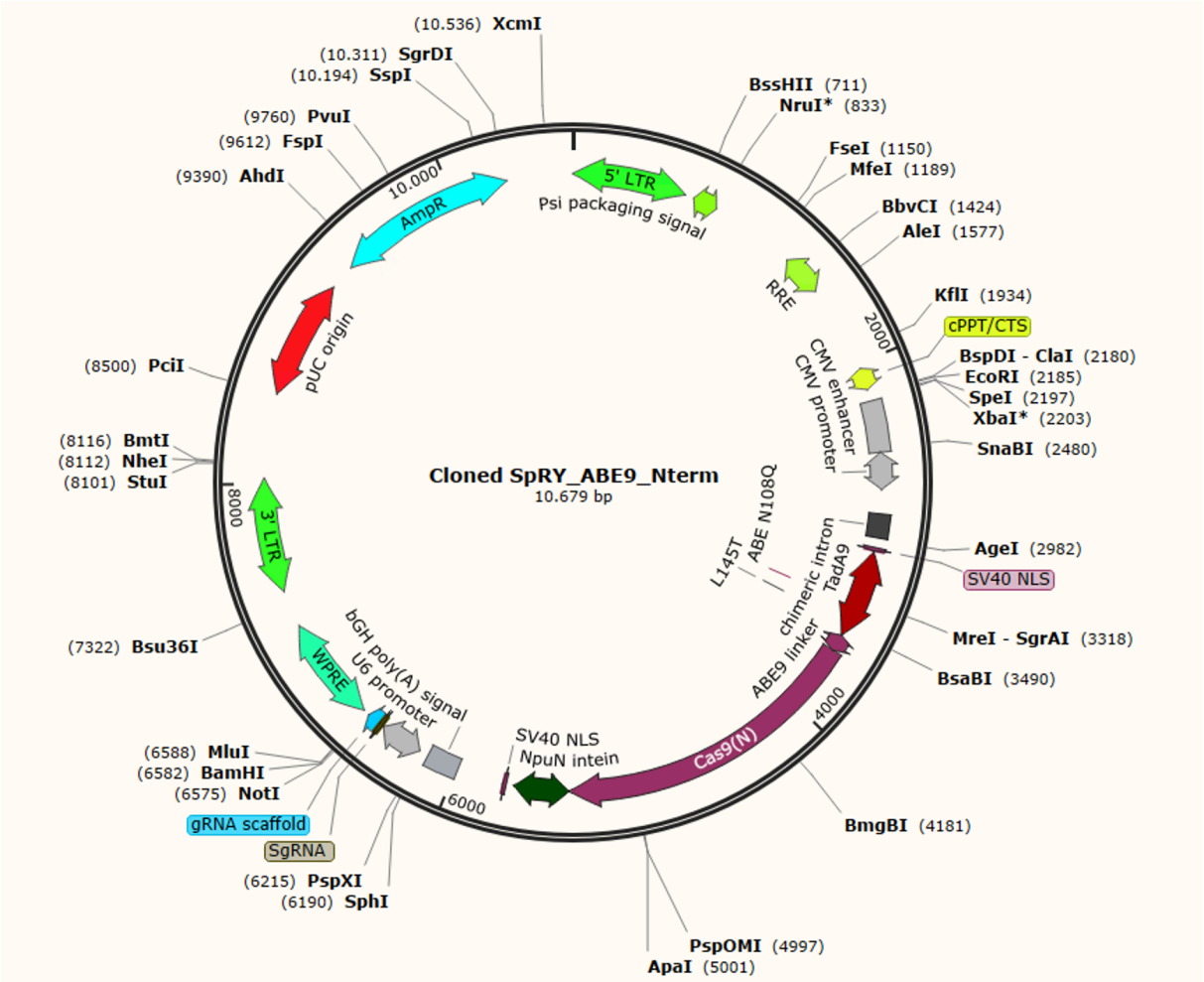

# Appendix 6: iABE-NGa-Cterm plasmid map (including sgRNA)

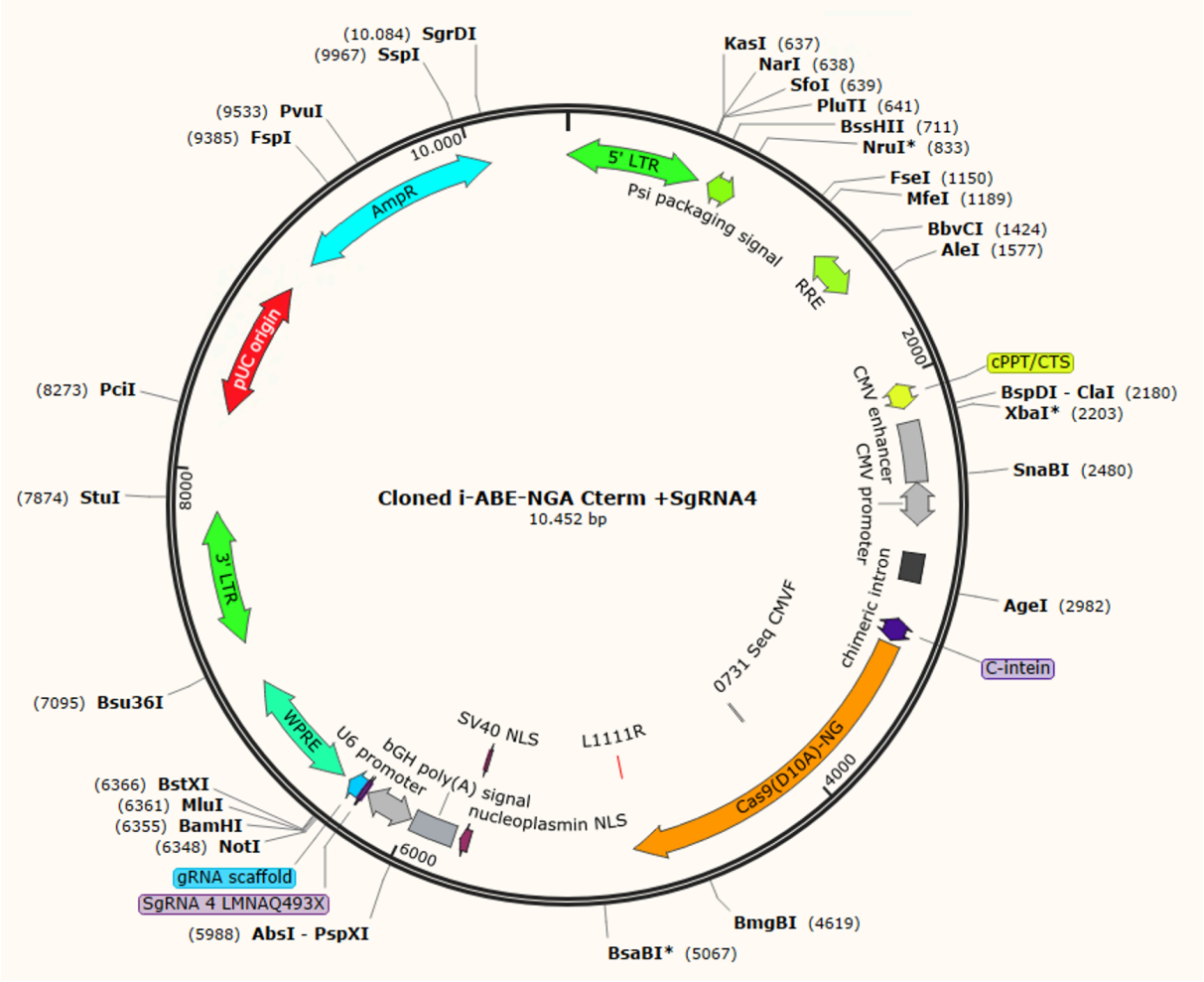

# Appendix 7: iABE-NGa-Nterm plasmid map (including sgRNA)

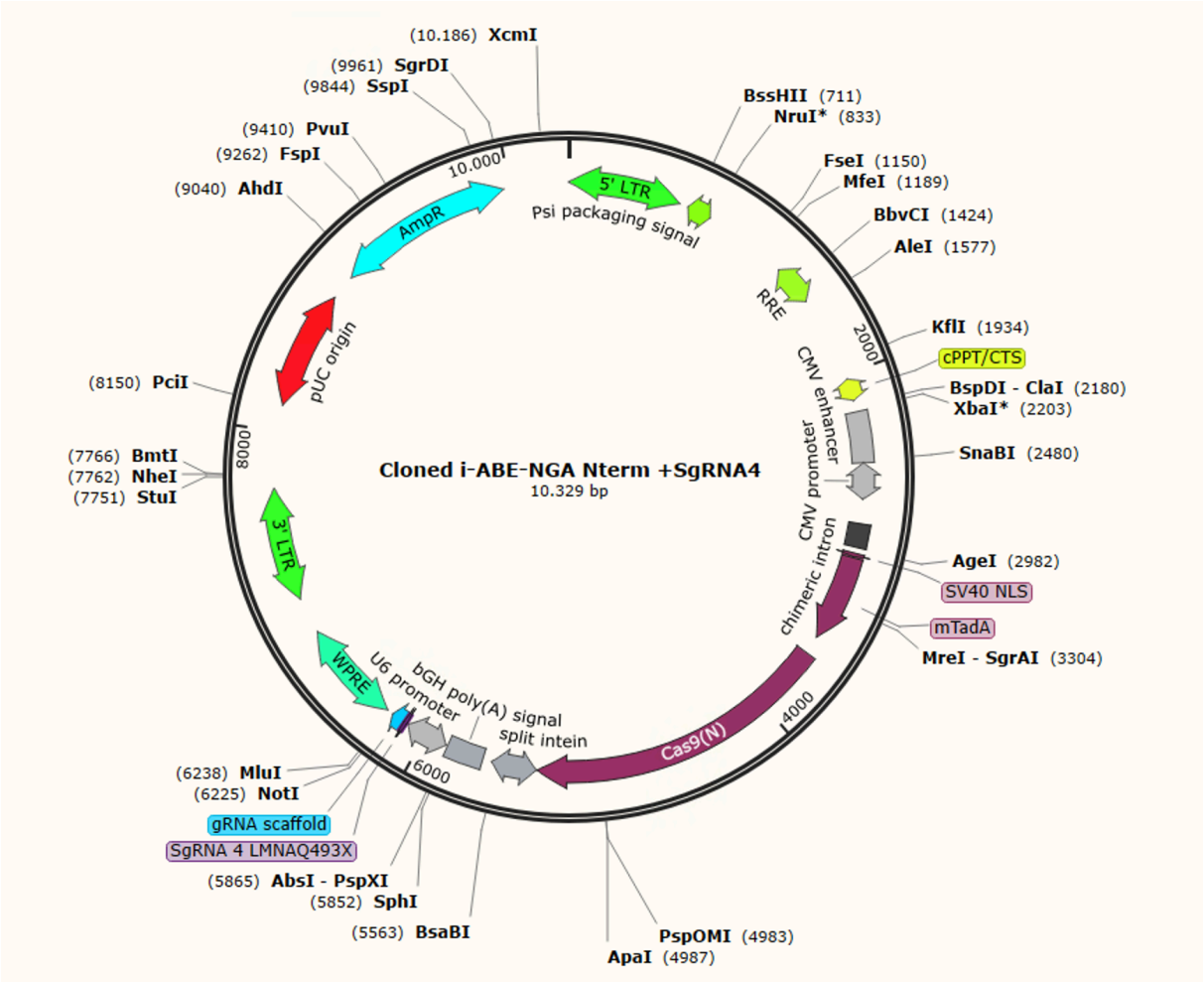

# Appendix 8: pMD2.G plasmid map

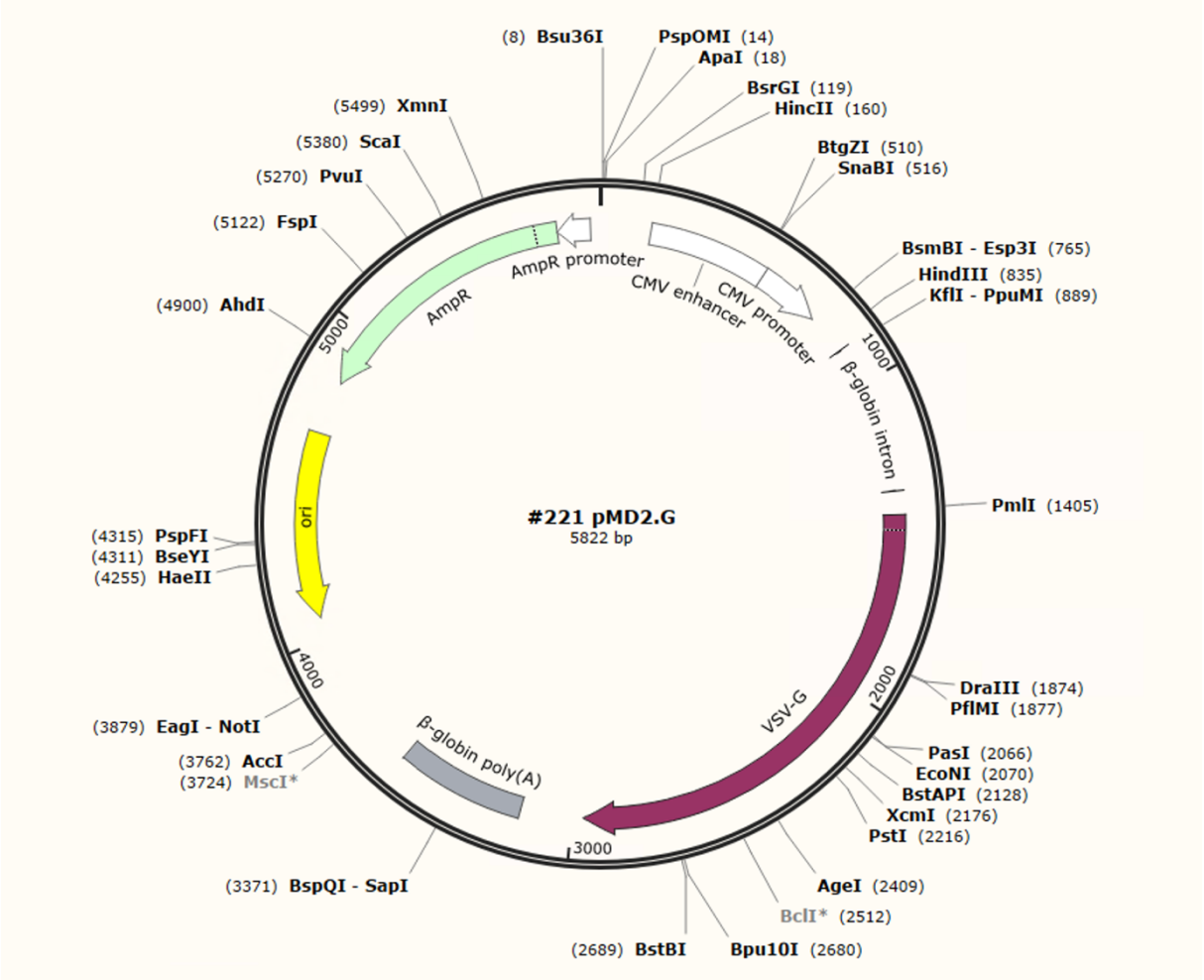

# Appendix 9: psPAX2 plasmid map

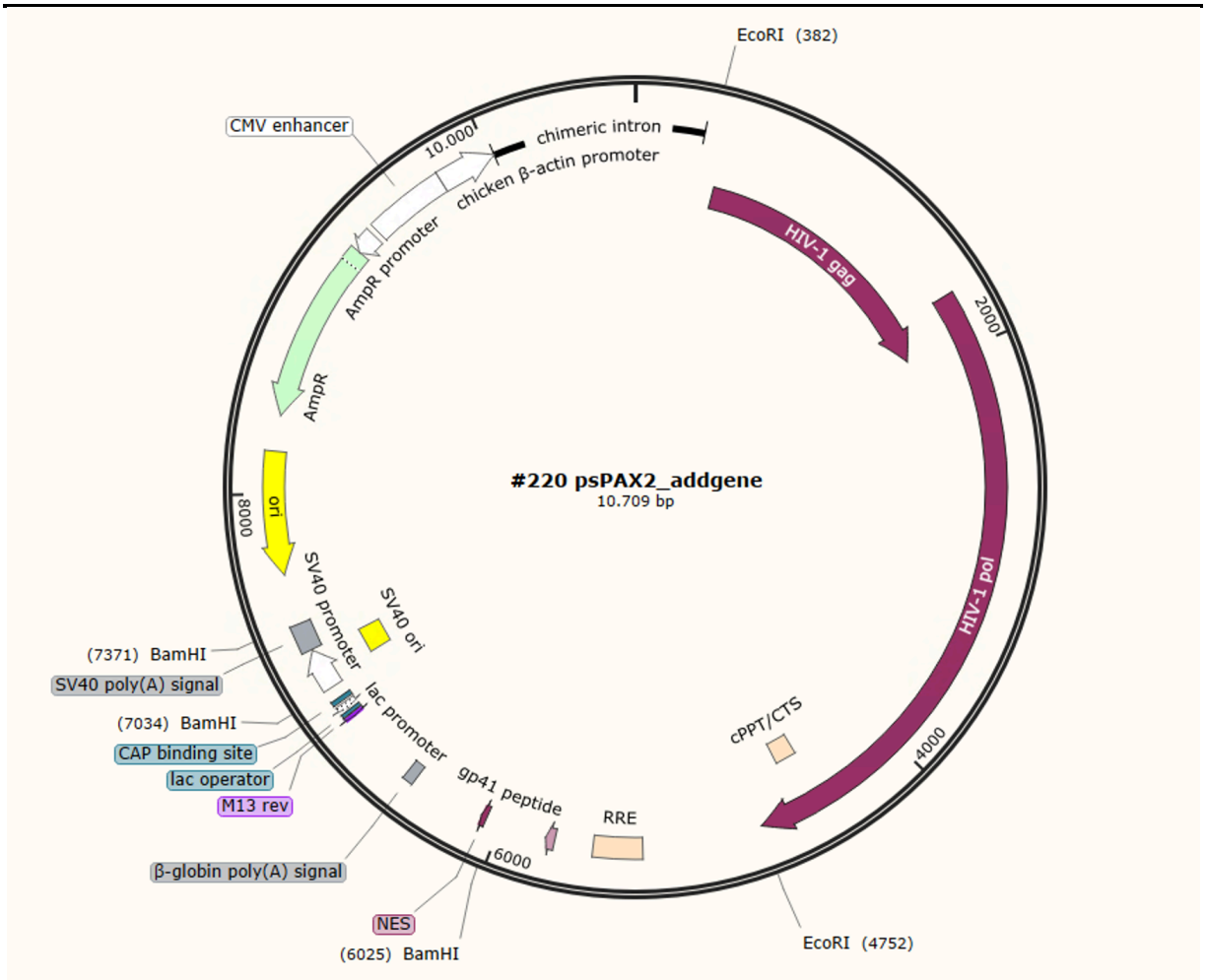

# References


1. Crasto S, My I, Di Pasquale E. The Broad Spectrum of LMNA Cardiac Diseases: From Molecular Mechanisms to Clinical Phenotype. Front Physiol. 2020;11(July):1–11.

2. McKenna WJ, Elliott PM. Diseases of the Myocardium and Endocardium. In: Goldman L, Schafer AI, editors. Goldman-Cecil Medicine. 26th ed. philadelphia: Elsevier; 2019. p. 297–314.

3. McNally EM, Mestroni L. Dilated cardiomyopathy: Genetic determinants and mechanisms. Circ Res . 2017;121(7):731–48.

4. Peretto G, Sala S, Benedetti S, Di Resta C, Gigli L, Ferrari M, et al. Updated clinical overview on cardiac laminopathies: an electrical and mechanical disease. Nucleus . 2018 Jan 1;9(1):380–91.

5. Taylor MRG, Fain PR, Sinagra G, Robinson ML, Robertson AD, Carniel E, et al. Natural history of dilated cardiomyopathy due to lamin A/C gene mutations. J Am Coll Cardiol. 2003 Mar 5;41(5):771–80.

6. van Rijsingen IAW, Nannenberg EA, Arbustini E, Elliott PM, Mogensen J, Hermans-van Ast JF, et al. Gender-specific differences in major cardiac events and mortality in lamin A/C mutation carriers. Eur J Heart Fail. 2013;15(4):376–84.

7. Tenga R, Medalia O. Structure and unique mechanical aspects of nuclear lamin filaments. sciencedirect . 2020;64:152–9.

8. Burke B, Stewart CL. The nuclear lamins : flexibility in function. Nat Rev Mol Cell Biol . 2013;14(January):29–31.

9. Davies BSJ, Coffinier C, Yang SH, Barnes RH, Jung H jin, Young SG, et al. Investigating the purpose of prelamin A processing. Landes bioscience . 2011;2(1):4–9.

10. Jeong S, Ahn J, Jo I, Kang S mi, Park B joon, Cho H soo, et al. Cyclin-dependent kinase 1 depolymerizes nuclear lamin filaments by disrupting the head-to-tail interaction of the lamin central rod domain. Journal of Biological Chemistry . 2022;298(9):1–10.

11. Ahn J, Jo I, Kang S mi, Hong S, Kim Y hak, Park B joon, et al. structural basis for lamin assembly at the molecular level. Nat Commun . 2019;10(3757):1–12.

12. Dubik N, Mai S. Lamin A / C : Function in Normal and Tumor Cells. Cancers (Basel) . 2020;12:1–21.

13. Crisp M, Liu Q, Roux K, Rattner JB, Shanahan C, Burke B, et al. Coupling of the nucleus and cytoplasm : role of the LINC complex. J Cell Biol . 2006;172(1):41–53.

14. Swift J, Ivanovska IL, Buxboim A, Harada T, Dave PCP, Pinter J, et al. Nuclear Lamin-A Scales with Tissue Stiffness and Enhances Matrix-Directed Differentiation. Science (1979) . 2013;341(6149):1–33.

15. Donnaloja F, Carnevali F, Jacchetti E, Raimondi MT. Lamin A / C Mechanotransduction in Laminopathies. Cells . 2020 May 24;9(5):1–33.

16. Gesson K, Rescheneder P, Skoruppa MP, Haeseler A Von, Dechat T, Foisner R. A-type lamins bind both hetero- and euchromatin , the latter being regulated by lamina-associated polypeptide 2 alpha. Genome Res . 2016;4:462–73.

17. Bronshtein I, Kepten E, Kanter I, Lindner M, Redwood AB, Mai S, et al. loss of lamin A function increases chromatin dynamics in the nuclear interior. Nat Commun. 2015;6:1–9.

18. Wood AM, Danielsen JMR, Lucas CA, Rice EL, Scalzo D, Shimi T, et al. TRF2 and Lamin A/C interact to facilitate the functional organization of chromosome ends. Nat Commun . 2014;5:1–9.

19. Spann TP, Goldman AE, Wang C, Huang S, Goldman RD. Alteration of nuclear lamin organization inhibits RNA polymerase II – dependent transcription. Journal of cell biology . 2002;156(4):603–8.

20. Nikolova V, Leimena C, McMahon AC, Tan JC, Chandar S, Jogia D, et al. Defects in nuclear structure and function promote dilated cardiomyopathy in lamin A/C–deficient mice. Journal of Clinical Investigation. 2004 Feb 1;113(3):357–69.

21. Chen CY, Chi YH, Mutalif RA, Starost MF, Myers TG, Anderson SA, et al. Accumulation of the inner nuclear envelope protein Sun1 is pathogenic in progeric and dystrophic laminopathies. Cell . 2012 Apr 1;149(3):565–77.

22. Mounkes LC, Kozlov S V., Rottman JN, Stewart CL. Expression of an LMNA-N195K variant of A-type lamins results in cardiac conduction defects and death in mice. Hum Mol Genet. 2005;14(15):2167–80.

23. Macquart C, Jüttner R, Morales Rodriguez B, Le Dour C, Lefebvre F, Chatzifrangkeskou M, et al. Microtubule cytoskeleton regulates Connexin 43 localization and cardiac conduction in cardiomyopathy caused by mutation in A-type lamins gene. Hum Mol Genet. 2019;28(24):4043–52.

24. Briand N, Collas P. Laminopathy-causing lamin A mutations reconfigure lamina-associated domains and local spatial chromatin conformation. Nucleus . 2018 Jan 1;9(1):216–26.

25. Cheedipudi SM, Matkovich SJ, Coarfa C, Hu X, Robertson MJ, Sweet M, et al. Genomic Reorganization of Lamin-Associated Domains in Cardiac Myocytes Is Associated With Differential Gene Expression and DNA Methylation in Human Dilated Cardiomyopathy. Circ Res . 2019 Apr 12;124(8):1198–213.

26. Morival JLP, Widyastuti HP, Nguyen CHH, Zaragoza M V., Downing TL. DNA methylation analysis reveals epimutation hotspots in patients with dilated cardiomyopathy-associated laminopathies. Clin Epigenetics . 2021 Dec 1;13(1):1–20.

27. Kubben N, Zhang W, Wang L, Voss TC, Yang J, Qu J, et al. Repression of the Antioxidant NRF2 Pathway in Premature Aging. Cell . 2016 Jun 2;165(6):1361–74.

28. Muchir A, Pavlidis P, Decostre V, Herron AJ, Arimura T, Bonne G, et al. Activation of MAPK pathways links LMNA mutations to cardiomyopathy in Emery-Dreifuss muscular dystrophy. J Clin Invest . 2007 May 1;117(5):1282–93.

29. Osmanagic-Myers S, Foisner R. The structural and gene expression hypotheses in laminopathic diseases - Not so different after all. Mol Biol Cell . 2019 Jul 15 ;30(15):1786–90.

30. Arimura T, Helbling-Leclerc A, Massart C, Varnous S, Niel F, Lacène E, et al. Mouse model carrying H222P-Lmna mutation develops muscular dystrophy and dilated cardiomyopathy similar to human striated muscle laminopathies. Hum Mol Genet . 2005 Jan 1;14(1):155–69.

31. Alter P, Waldhans S, Plachta E, Moosdorf R, Grimm W. Complications of Implantable Cardioverter Defibrillator Therapy in 440 Consecutive Patients. Pacing and Clinical Electrophysiology . 2005 Sep 1;28(9):926–32.

32. Potena L, Zuckermann A, Barberini F, Aliabadi-Zuckermann A. Complications of Cardiac Transplantation. Curr Cardiol Rep . 2018 Sep 1;20(9):1–11.

33. Muchir A, Wu W, Choi JC, Iwata S, Morrow J, Homma S, et al. Abnormal p38α mitogen-activated protein kinase signaling in dilated cardiomyopathy caused by lamin A/C gene mutation. Hum Mol Genet . 2012 Oct 1;21(19):4325–33.

34. Choi JC, Muchir A, Wu W, Iwata S, Homma S, Morrow JP, et al. Temsirolimus activates autophagy and ameliorates cardiomyopathy caused by lamin A/C gene mutation. Sci Transl Med. 2012;4(144):1–9.

35. Wu W, Muchir A, Shan J, Bonne G, Worman HJ. Mitogen-activated protein kinase inhibitors improve heart function and prevent fibrosis in cardiomyopathy caused by mutation in Lamin A/C gene. Circulation. 2011 Jan 4;123(1):53–61.

36. Judge DP, Taylor MRG, Li H, Oliver C, Angeli FS, Lee PA, et al. Long-term effectiveness of ARRY-371797 in people with dilated cardiomyopathy and a faulty LMNA gene: a plain language summary. Future Cardiol. 2023 Mar 1;19(3):117–26.

37. Garcia-Pavia P, Palomares JFR, Sinagra G, Barriales-Villa R, Lakdawala NK, Gottlieb RL, et al. REALM-DCM: A Phase 3, Multinational, Randomized, Placebo-Controlled Trial of ARRY-371797 in Patients With Symptomatic LMNA -Related Dilated Cardiomyopathy. Circ Heart Fail. 2024 Jul;17(7):e011548.

38. Salvarani N, Crasto S, Miragoli M, Bertero A, Paulis M, Kunderfranco P, et al. The K219T-Lamin mutation induces conduction defects through epigenetic inhibition of SCN5A in human cardiac laminopathy. Nat Commun. 2019 Dec 1;10(1):1–16.

39. Frock RL, Chen SC, Da DF, Frett E, Lau C, Brown C, et al. Cardiomyocyte-specific expression of lamin A improves cardiac function in Lmna-/- mice. PLoS One. 2012;7(8):e42918.

40. Scharner J, Figeac N, Ellis JA, Zammit PS. Ameliorating pathogenesis by removing an exon containing a missense mutation: A potential exon-skipping therapy for laminopathies. Gene Ther. 2015;22(6):503–15.

41. Reichart D, Newby GA, Wakimoto H, Lun M, Gorham JM, Curran JJ, et al. Efficient in vivo genome editing prevents hypertrophic cardiomyopathy in mice. Nat Med. 2023 Feb 1;29(2):412–21.

42. Ma S, Jiang W, Liu X, Lu WJ, Qi T, Wei J, et al. Efficient Correction of a Hypertrophic Cardiomyopathy Mutation by ABEmax-NG. Circ Res. 2021 Oct 29;129(10):895–908.

43. Chai AC, Cui M, Chemello F, Li H, Chen K, Tan W, et al. Base editing correction of hypertrophic cardiomyopathy in human cardiomyocytes and humanized mice. Nat Med. 2023 Feb 1;29(2):401–11.

44. Grosch M, Schraft L, Chan A, Küchenhoff L, Rapti K, Ferreira AM, et al. Striated muscle-specific base editing enables correction of mutations causing dilated cardiomyopathy. Nat Commun. 2023 Dec 1;14(1):3714.

45. Nishiyama T, Zhang Y, Cui M, Li H, Sanchez-Ortiz E, McAnally JR, et al. Precise genomic editing of pathogenic mutations in RBM20 rescues dilated cardiomyopathy. Sci Transl Med. 2022 Nov 23;14(672):eade1633.

46. Rees HA, Liu DR. Base editing: precision chemistry on the genome and transcriptome of living cells. Nat Rev Genet. 2018 Dec 1;19(12):770–88.

47. Gaudelli NM, Komor AC, Rees HA, Packer MS, Badran AH, Bryson DI, et al. Programmable base editing of T to G C in genomic DNA without DNA cleavage. Nature. 2017 Nov 23;551(7681):464–71.

48. Song M, Kim HK, Lee S, Kim Y, Seo SY, Park J, et al. Sequence-specific prediction of the efficiencies of adenine and cytosine base editors. Nat Biotechnol. 2020 Sep 1;38(9):1037–43.

49. Yang L, Liu Z, Sun J, Chen Z, Gao F, Guo Y. Adenine base editor-based correction of the cardiac pathogenic Lmna c.1621C > T mutation in murine hearts. J Cell Mol Med. 2024 Feb 1;28(4):e18145.

50. Hu JH, Miller SM, Geurts MH, Tang W, Chen L, Sun N, et al. Evolved Cas9 variants with broad PAM compatibility and high DNA specificity. Nature. 2018 Apr 5;556(7699):57–63.

51. Yang L, Zhang X, Wang L, Yin S, Zhu B, Xie L, et al. Increasing targeting scope of adenosine base editors in mouse and rat embryos through fusion of TadA deaminase with Cas9 variants. Protein Cell. 2018 Sep 1;9(9):814–9.

52. Kleinstiver BP, Prew MS, Tsai SQ, Nguyen NT, Topkar V V., Zheng Z, et al. Broadening the targeting range of Staphylococcus aureus CRISPR-Cas9 by modifying PAM recognition. Nat Biotechnol. 2015 Dec 1;33(12):1293–8.

53. Kleinstiver BP, Prew MS, Tsai SQ, Topkar V V., Nguyen NT, Zheng Z, et al. Engineered CRISPR-Cas9 nucleases with altered PAM specificities. Nature. 2015 Jul 23;523(7561):481–5.

54. Koblan LW, Doman JL, Wilson C, Levy JM, Tay T, Newby GA, et al. Improving cytidine and adenine base editors by expression optimization and ancestral reconstruction. Nat Biotechnol. 2018 Oct 1;36(9):843–8.

55. Liu Z, Chen M, Shan H, Chen S, Xu Y, Song Y, et al. Expanded targeting scope and enhanced base editing efficiency in rabbit using optimized xCas9(3.7). Cellular and Molecular Life Sciences. 2019 Oct 1;76(20):4155–64.

56. Rees HA, Wilson C, Doman JL, Liu DR. Analysis and minimization of cellular RNA editing by DNA adenine base editors Adenine base editors (ABEs) enable precise and efficient conversion of target A•T base pairs to G·C base pairs in genomic DNA with a minimum of by-products. Sci Adv . 2019;5(5):eaax5717.

57. Zhou C, Sun Y, Yan R, Liu Y, Zuo E, Gu C, et al. Off-target RNA mutation induced by DNA base editing and its elimination by mutagenesis. Nature. 2019 Jul 11;571(7764):275–8.

58. Grünewald J, Zhou R, Iyer S, Lareau CA, Garcia SP, Aryee MJ, et al. CRISPR DNA base editors with reduced RNA off-target and self-editing activities. Nat Biotechnol. 2019 Sep 1;37(9):1041–8.

59. Richter MF, Zhao KT, Eton E, Lapinaite A, Newby GA, Thuronyi BW, et al. Phage-assisted evolution of an adenine base editor with improved Cas domain compatibility and activity. Nat Biotechnol. 2020 Jul 1;38(7):883–91.

60. Davis JR, Wang X, Witte IP, Huang TP, Levy JM, Raguram A, et al. Efficient in vivo base editing via single adeno-associated viruses with size-optimized genomes encoding compact adenine base editors. Nat Biomed Eng. 2022 Nov 1;6(11):1272–83.

61. Walton RT, Christie KA, Whittaker MN, Kleinstiver BP. Unconstrained genome targeting with near-PAMless engineered CRISPR-Cas9 variants. Science368 . 2020 Apr 17;368(6488):290–6.

62. Li G, Cheng Y, Li Y, Ma H, Pu Z, Li S, et al. A novel base editor SpRY-ABE8eF148A mediates efficient A-to-G base editing with a reduced off-target effect. Mol Ther Nucleic Acids. 2023 Mar 14;31:78–87.

63. Jeong YK, Lee SH, Hwang GH, Hong SA, Park S eun, Kim JS, et al. Adenine base editor engineering reduces editing of bystander cytosines. Nat Biotechnol. 2021 Nov 1;39(11):1426–33.

64. Liu Y, Zhou J, Lan T, Zhou X, Yang Y, Li C, et al. Elimination of Cas9-dependent off-targeting of adenine base editor by using TALE to separately guide deaminase to target sites. Cell Discov. 2022 Dec 1;8(28):1–5.

65. Zhang H, Bamidele N, Liu P, Ojelabi O, Gao XD, Rodriguez T, et al. Adenine Base Editing In Vivo with a Single Adeno-Associated Virus Vector . GEN Biotechnology. 2022 Jun 1;1(3):285–99.

66. Kweon J, Jang AH, Kwon E, Kim U, Shin HR, See J, et al. Targeted dual base editing with Campylobacter jejuni Cas9 by single AAV-mediated delivery. Exp Mol Med. 2023 Feb 1;55(2):377–84.

67. Chen L, Zhang S, Xue N, Hong M, Zhang X, Zhang D, et al. Engineering a precise adenine base editor with minimal bystander editing. Nat Chem Biol. 2023 Jan 1;19(1):101–10.

68. Chen F, Lian M, Ma B, Gou S, Luo X, Yang K, et al. Multiplexed base editing through Cas12a variant-mediated cytosine and adenine base editors. Commun Biol. 2022 Dec 1;5(1163):1–12.

69. Zhang S, Song L, Yuan B, Zhang C, Cao J, Chen J, et al. TadA reprogramming to generate potent miniature base editors with high precision. Nat Commun. 2023 Dec 1;14(413):1–12.

70. Zhao D, Qian Y, Li J, Li Z, Lai L. Highly efficient A-to-G base editing by ABE8.17 in rabbits. Mol Ther Nucleic Acids. 2022 Mar 8;27:1156–63.

71. Huang TP, Heins ZJ, Miller SM, Wong BG, Balivada PA, Wang T, et al. High-throughput continuous evolution of compact Cas9 variants targeting single-nucleotide-pyrimidine PAMs. Nat Biotechnol. 2023 Jan 1;41(1):96–107.

72. Bamidele N, Zhang H, Dong X, Cheng H, Gaston N, Feinzig H, et al. Domain-inlaid Nme2Cas9 adenine base editors with improved activity and targeting scope. Nat Commun. 2024 Dec 1;15(1458):1–13.

73. Xu L, Zhang C, Li H, Wang P, Gao Y, Mokadam NA, et al. Efficient precise in vivo base editing in adult dystrophic mice. Nat Commun. 2021 Dec 1;12(3719):1–14.

74. Su J, Jin X, She K, Liu Y, Song L, Zhao Q, et al. In vivo adenine base editing corrects newborn murine model of Hurler syndrome. Molecular Biomedicine. 2023 Dec 1;4(6):1–14.

75. Liang F, Zhang Y, Li L, Yang Y, Fei JF, Liu Y, et al. SpG and SpRY variants expand the CRISPR toolbox for genome editing in zebrafish. Nat Commun. 2022 Dec 1;13(3421):1–10.

76. Karvelis T, Gasiunas G, Siksnys V. Methods for decoding Cas9 protospacer adjacent motif (PAM) sequences: A brief overview. Methods. 2017 May 15;121–122:3–8.

77. Wivel NA, Wilson JM. METHODS OF GENE DELIVERY. Hematol Oncol Clin North Am. 1998 Jun 1;12(3):483–501.

78. Djurovic S, Iversen N, Jeansson S, Hoover F, Christensen G. Abstract Comparison of Nonviral Transfection and Adeno-Associated Viral Transduction on Cardiomyocytes. Mol Biotechnol. 2004 Sep;28:21–31.

79. Bouard D, Alazard-Dany N, Cosset FL. Viral vectors: From virology to transgene expression. Br J Pharmacol. 2009 May;157(2):153–65.

80. Gao GP, Alvira MR, Wang L, Calcedo R, Johnston J, Wilson JM. Novel adeno-associated viruses from rhesus monkeys as vectors for human gene therapy. Proceedings of the National Academy of Sciences . 2002 Sep 3;99(18):11854–9.

81. Bainbridge JWB, Smith AJ, Barker SS, Robbie S, Henderson R, Balaggan K, et al. Effect of Gene Therapy on Visual Function in Leber's Congenital Amaurosis. New England Journal of Medicine. 2008 May 22;358(21):2231–9.

82. Podsakoff G, Wong KK, Chatterjeei S. Efficient Gene Transfer into Nondividing Cells by Adeno-Associated Virus-Based Vectors. J Virol . 1994 Sep;68(9):5656–66.

83. Schnepp BC, Clark KR, Klemanski DL, Pacak CA, Johnson PR. Genetic Fate of Recombinant Adeno-Associated Virus Vector Genomes in Muscle. J Virol. 2003 Mar 15;77(6):3495–504.

84. Zincarelli C, Soltys S, Rengo G, Rabinowitz JE. Analysis of AAV serotypes 1-9 mediated gene expression and tropism in mice after systemic injection. Molecular Therapy. 2008;16(6):1073–80.

85. Wang Z, Zhu T, Qiao C, Zhou L, Wang B, Zhang J, et al. Adeno-associated virus serotype 8 efficiently delivers genes to muscle and heart. Nat Biotechnol. 2005 Mar;23(3):321–8.

86. Schröder LC, Frank D, Müller OJ. Transcriptional Targeting Approaches in Cardiac Gene Transfer Using AAV Vectors. Pathogens. 2023 Nov 1;12(11):1–13.

87. Liu GH, Suzuki K, Qu J, Sancho-Martinez I, Yi F, Li M, et al. Targeted gene correction of laminopathy-associated LMNA mutations in patient-specific iPSCs. Cell Stem Cell. 2011 Jun 3;8(6):688–94.

88. Koblan LW, Erdos MR, Wilson C, Cabral WA, Levy JM, Xiong ZM, et al. In vivo base editing rescues Hutchinson–Gilford progeria syndrome in mice. Nature. 2021 Jan 28;589(7843):608–14.

89. Al-Saaidi R, Rasmussen TB, Palmfeldt J, Nissen PH, Beqqali A, Hansen J, et al. The LMNA mutation p.Arg321Ter associated with dilated cardiomyopathy leads to reduced expression and a skewed ratio of lamin A and lamin C proteins. Exp Cell Res. 2013 Nov 15;319(19):3010–9.

90. Fairley EAL, Riddell A, Ellis JA, Kendrick-Jones. John. The cell cycle dependent mislocalisation of emerin may contribute to the Emery-Dreifuss muscular dystrophy phenotype. Journal of Cell Science . 2002 Jan 15;115(2):341–54.

91. Reunert J, Wentzell R, Walter M, Jakubiczka S, Zenker M, Brune T, et al. Neonatal progeria: Increased ratio of progerin to lamin A leads to progeria of the newborn. European Journal of Human Genetics. 2012 Sep;20(9):933–7.

92. Al-Saaidi R, Bross P. Do lamin A and lamin C have unique roles? Chromosoma. 2015 Mar 1;124(1):1–2.

93. Larson MG. Analysis of variance. Circulation. 2008 Jan;117(1):115–21.

94. Kumar S, Nagesh D, Ramasubbu V, Prabhashankar AB, Sundaresan NR. Isolation and Culture of Primary Fibroblasts from Neonatal Murine Hearts to Study Cardiac Fibrosis. Bio Protoc. 2023 Feb 20;13(4):1–18.

95. Uhlén M, Fagerberg L, Hallström B, M. Lindskog C, Oksvold P, Määttä T, et al. Human protein atlas. 2023. Image: single cell RNA data on LMNA in liver tissue available from v23.proteinatlas.org.

96. Oey H, Isbel L, Hickey P, Ebaid B, Whitelaw E. Genetic and epigenetic variation among inbred mouse littermates: Identification of inter-individual differentially methylated regions. Epigenetics Chromatin. 2015 Dec 12;8(54):1–12.

97. Chebib J, Jackson BC, López-Cortegano E, Tautz D, Keightley PD. Inbred lab mice are not isogenic: genetic variation within inbred strains used to infer the mutation rate per nucleotide site. Heredity (Edinb). 2021 Jan 1;126(1):107–16.

98. Baranyi U, Winter B, Gugerell A, Hegedus B, Brostjan C, Laufer G, et al. Primary human fibroblasts in culture switch to a myofibroblast-like phenotype independently of TGF beta. Cells. 2019 Jul 13;8(7):1–16.

99. Landry NM, Rattan SG, Dixon IMC. An Improved Method of Maintaining Primary Murine Cardiac Fibroblasts in Two-Dimensional Cell Culture. Sci Rep. 2019 Sep 9;9(12889):1–13.

100. Wang Y, Yoshitomi T, Kawazoe N, Yang Y, Chen G. Micropattern-Controlled Cell Density and Its Effect on Gene Transfection of Mesenchymal Stem Cells. Adv Mater Interfaces. 2022 Jan 27;9(2101978):1–13.

101. Rogers AB, Dintzis RZ. Hepatobiliary System. In: Treuting PM, Dintzis SM, Montine KS, editors. Comparative Anatomy and Histology. 2nd ed. Cambridge: Academic press; 2018. p. 229–39.

102. Baratta JL, Ngo A, Lopez B, Kasabwalla N, Longmuir KJ, Robertson RT. Cellular organization of normal mouse liver: A histological, quantitative immunocytochemical, and fine structural analysis. Histochem Cell Biol. 2009 Jun;131(6):713–26.

103. Rubin H. Cell aging in vivo and in vitro. Mech Ageing Dev. 1997 Oct;98(1):1–35.

104. May T, Mueller PP, Weich H, Froese N, Deutsch U, Wirth D, et al. Establishment of murine cell lines by constitutive and conditional immortalization. J Biotechnol. 2005 Oct 17;120(1):99–110.

105. Su K, Wu Z, Wu H. Simulation, power evaluation and sample size recommendation for single-cell RNA-seq. Bioinformatics. 2020 Oct 1;36(19):4860–8.

106. Gehrke JM, Cervantes O, Clement MK, Pinello L, Joung JK. High-precision CRISPR-Cas9 base editors with minimized bystander and off-target mutations. bioRxiv . 2018 Mar 1;1–22.

107. Wang Q, Yang J, Zhong Z, Vanegas JA, Gao X, Kolomeisky AB. A general theoretical framework to design base editors with reduced bystander effects. Nat Commun. 2021 Dec 1;12(6529):1–10.

108. Gupta AK, Gupta UD. Next generation sequencing and its applications. In: Verma AS, Singh A, editors. Animal Biotechnology . 2nd ed. Cambridge: Academic Press; 2020. p. 395–421.

109. Maggi L, Carboni N, Bernasconi P. Skeletal Muscle Laminopathies: A Review of Clinical and Molecular Features. Cells . 2016 Aug 11;5(3):33.

110. Behr M, Zhou J, Xu B, Zhang H. In vivo delivery of CRISPR-Cas9 therapeutics: Progress and challenges. Acta Pharm Sin B. 2021 Aug 1;11(8):2150–71.

111. Singh AM, Steffey VVA, Yeshi T, Allison DW, Singh AM, Or Allison DW. Gene Editing in Human Pluripotent Stem Cells: Choosing the Correct Path. J Stem Cell Regen Biol. 2015 Nov 5;1(1):1–9.

112. Dixit S, Kumar A, Srinivasan K, Vincent PMDR, Ramu Krishnan N. Advancing genome editing with artificial intelligence: opportunities, challenges, and future directions. Front Bioeng Biotechnol. 2024 Jan 8;11:1–16.

113. Prykhozhij S V., Rajan V, Berman JN. A Guide to Computational Tools and Design Strategies for Genome Editing Experiments in Zebrafish Using CRISPR/Cas9. Zebrafish. 2016 Feb 1;13(1):70–3.

114. Balakrishnan M, Kotla A, Agarwal S, Krishnan P, Supriya P, Srinivasa Rao C. Computational tools and scientometrics for CRISPR-based genome editing. J Plant Biochem Biotechnol. 2023 Dec 1;32(4):808–17.

115. Daneshpajouh A, Fowler M, Wiese KC. Navitas/Optimus: A Novel Computational Tool for enhanced CRISPR/Cas Genome Editing. In: 36th Canadian AI. 2023.